Viscoelasticity and Collective Cell Migration

An interdisciplinary perspective across levels of organization

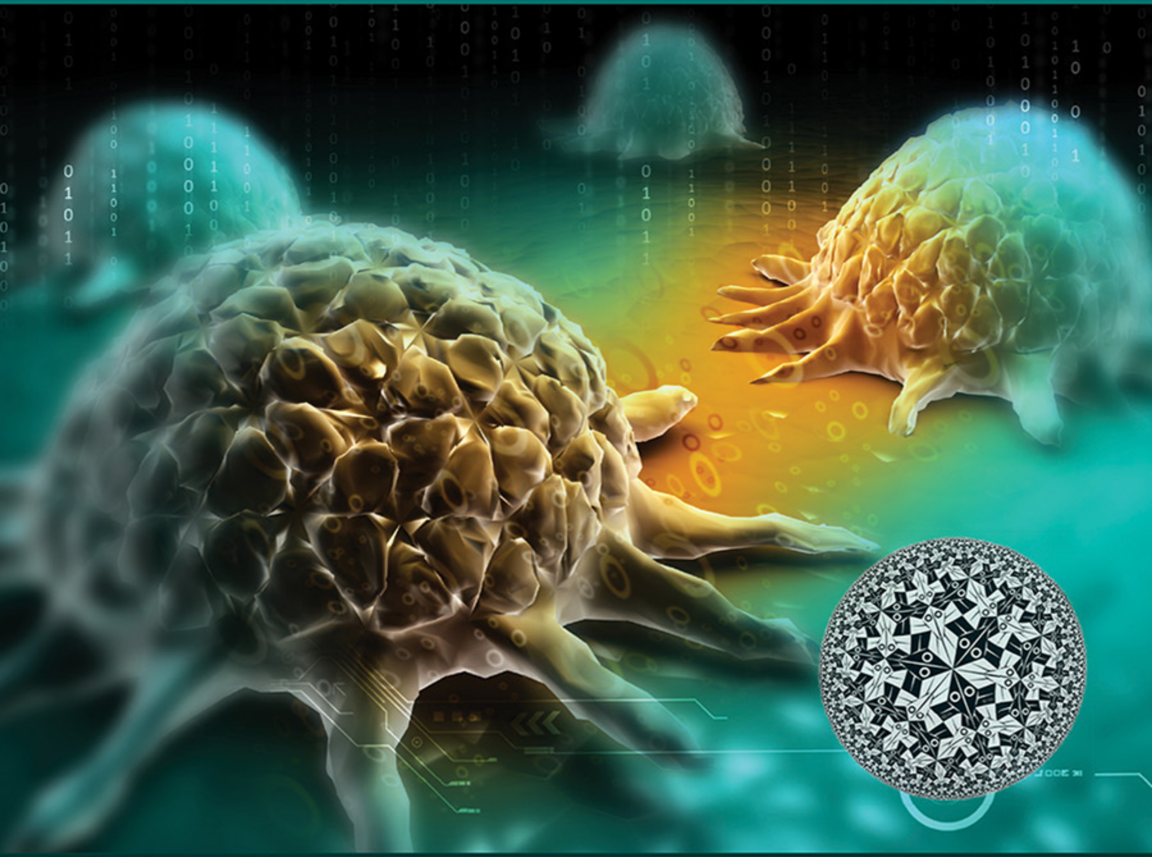

Edited by
Ivana Pajic-Lijakovic
Elias H Barriga

VISCOELASTICITY AND COLLECTIVE CELL MIGRATION

VISCOELASTICITY AND COLLECTIVE CELL MIGRATION

An Interdisciplinary Perspective Across Levels of Organization

Edited by

IVANA PAJIC-LIJAKOVIC
Laboratoire Interdisciplinaire de Physique, CNRS,
Université Grenoble Alpes, Grenoble, France

ELIAS H BARRIGA
Mechanisms of Morphogenesis Lab, Gulbenkian Institute
of Science (IGC), Oeiras, Portugal

ELSEVIER

ACADEMIC PRESS
An imprint of Elsevier

Academic Press is an imprint of Elsevier
125 London Wall, London EC2Y 5AS, United Kingdom
525 B Street, Suite 1650, San Diego, CA 92101, United States
50 Hampshire Street, 5th Floor, Cambridge, MA 02139, United States
The Boulevard, Langford Lane, Kidlington, Oxford OX5 1GB, United Kingdom

Copyright © 2021 Elsevier Inc. All rights reserved.

No part of this publication may be reproduced or transmitted in any form or by any means, electronic or mechanical, including photocopying, recording, or any information storage and retrieval system, without permission in writing from the publisher. Details on how to seek permission, further information about the Publisher's permissions policies and our arrangements with organizations such as the Copyright Clearance Center and the Copyright Licensing Agency, can be found at our website: www.elsevier.com/permissions.

This book and the individual contributions contained in it are protected under copyright by the Publisher (other than as may be noted herein).

Notices
Knowledge and best practice in this field are constantly changing. As new research and experience broaden our understanding, changes in research methods, professional practices, or medical treatment may become necessary.

Practitioners and researchers must always rely on their own experience and knowledge in evaluating and using any information, methods, compounds, or experiments described herein. In using such information or methods they should be mindful of their own safety and the safety of others, including parties for whom they have a professional responsibility.

To the fullest extent of the law, neither the Publisher nor the authors, contributors, or editors, assume any liability for any injury and/or damage to persons or property as a matter of products liability, negligence or otherwise, or from any use or operation of any methods, products, instructions, or ideas contained in the material herein.

British Library Cataloguing-in-Publication Data
A catalogue record for this book is available from the British Library

Library of Congress Cataloging-in-Publication Data
A catalog record for this book is available from the Library of Congress

ISBN: 978-0-12-820310-1

For Information on all Academic Press publications
visit our website at https://www.elsevier.com/books-and-journals

Publisher: Mara Conner
Acquisitions Editor: Fiona Geraghty
Editorial Project Manager: Charlotte Rowley
Production Project Manager: Sojan P. Pazhayattil
Cover Designer: Victoria Pearson

Typeset by MPS Limited, Chennai, India

ELSEVIER
Book Aid International
Working together
to grow libraries in
developing countries
www.elsevier.com • www.bookaid.org

Contents

List of Contributors *ix*

1. The basics of collective cell migration: unity makes strength **1**

Joana E. Saraiva and Elias H. Barriga

1.1 Introduction 1
1.2 Experimental models to study collective cell migration 2
1.3 Using cell—cell junctions to stay as a group and communicate 7
1.4 Future perspectives 12
Acknowledgments 13
References 13

2. The basic concept of viscoelasticity **21**

Ivana Pajic-Lijakovic

2.1 Introduction 21
2.2 Linear viscoelasticity: constitutive models 23
2.3 Characteristics of the jamming state as the nonlinear viscoelastic solid 31
2.4 The main characteristics of various viscoelastic models 36
2.5 Relaxation of multicellular systems under externally applied stress conditions 38
2.6 Conclusions 42
Acknowledgment 43
References 43

3. Biophysical origins of viscoelasticity during collective cell migration **47**

Andrew G. Clark

3.1 Introduction 47
3.2 Timescale-dependent behavior in viscoelastic materials 48
3.3 Measuring viscoelastic behavior in biology 49
3.4 Viscoelasticity of the actin cytoskeleton 54
3.5 Cell—substrate adhesions and force transmission during migration 59
3.6 Substrate mechanics during migration 61
3.7 Cell—cell adhesion dynamics 64
3.8 Viscoelasticity in collective tissue migration 66

3.9 Conclusion 69
Acknowledgments 69
References 70

4. Fine-tuning viscoelasticity: the key to collectively move in vivo 79
Jaime A. Espina and Elias H. Barriga

4.1 Introduction 79
4.2 Viscoelasticity of cellular components 80
4.3 Sensing and transducing environmental viscoelasticity 84
4.4 Environmental viscoelasticity triggers and directs collective migration 93
4.5 Concluding remarks and future perspectives 97
Acknowledgments 98
References 98

5. Effects of time delays and viscoelastic parameters in oscillatory response of cell monolayers 111
Cristian Borja, Elena Moral and Jose J. Muñoz

5.1 Introduction 111
5.2 Planar deformations 112
5.3 Analysis of tissue cross-section 124
5.4 Conclusions 130
Acknowledgments 131
References 131

6. Viscoelastic properties driving collective migration in zebrafish development 135
Timo Betz

6.1 Introduction 135
6.2 Morphogenesis and zebrafish development 137
6.3 Epiboly 140
6.4 Doming 147
6.5 Gastrulation 148
6.6 Somite formation 150
6.7 Outlook 152
References 154

7. Oscillations in collective cell migration **157**

Vanni Petrolli, Thomas Boudou, Martial Balland and Giovanni Cappello

7.1 Introduction 157
7.2 Mechanism of collective cell motion 158
7.3 Propagative waves 160
7.4 Standing waves in fully confined monolayers 170
7.5 Mechanical considerations 177
7.6 Discussion 181
7.7 Conclusion and perspective 183
References 186

8. Flow dynamics of 3D multicellular systems into capillaries **193**

Karine Guevorkian, Françoise Brochard-Wyart and
David Gonzalez-Rodriguez

8.1 Introduction 193
8.2 Micropipette aspiration technique: a practical guide 194
8.3 Viscoelastic behavior of cellular aggregates 200
8.4 Active response of cellular aggregates to mechanical stimuli 210
8.5 Permeability of cellular aggregates 215
8.6 Conclusions and perspectives 219
Acknowledgments 220
References 220

9. Viscoelasticity of multicellular systems caused by collective cell migration: multiscale modeling considerations **225**

Ivana Pajic-Lijakovic and Milan Milivojevic

9.1 Introduction 225
9.2 Phenomenological description of long-time rearrangement of multicellular surfaces under external stress 227
9.3 Long-time viscoelasticity at a mesoscopic level—constitutive modeling 230
9.4 Long-time viscoelasticity at a macroscopic level—constitutive modeling 239
9.5 Conclusion 250
Acknowledgment 251
Declaration of interest 251
Appendix 1 251
Appendix 2 252
References 253

10. Recent advances in imaging of cell elasticity **257**

Teckla Akinyi, Pol Grasland-Mongrain, Manish Bhatt,
Stefan Catheline and Guy Cloutier

10.1 Introduction 257
10.2 Cell structure: key architectural players in elasticity 260
10.3 Estimation of cell elasticity 264
10.4 Rheological modeling of a single cell 272
10.5 Trends in viscoelastography 283
10.6 Summary 286
Acknowledgment 287
References 287

Index *297*

CHAPTER TEN

Recent advances in imaging of cell elasticity

Teckla Akinyi[1], Pol Grasland-Mongrain[2], Manish Bhatt[1], Stefan Catheline[3] and Guy Cloutier[1,4]
[1]Laboratory of Biorheology and Medical Ultrasonics, University of Montreal Hospital Research Center, Montréal, QC, Canada
[2]ENS de Lyon, Université Claude Bernard, CNRS, Laboratoire de Physique, Lyon, France
[3]LabTAU, INSERM unit 1032, Université de Lyon, Lyon, France
[4]Department of Radiology, Radio-oncology and Nuclear Medicine, and Institute of Biomedical Engineering, University of Montreal, Montréal, QC, Canada

10.1 Introduction

Biological cells have a complex chemical and mechanical environment upon which function and structural integrity rely. In performing their normal functions, cells adhere and spread on the extracellular matrix (ECM) to form tissues and collectively or individually migrate to the injured site during immune response. Depending on the functional state or in response to external stimuli, the mechanical properties of cells can change. These changes are mitigated by the rearrangement of subcellular structures and their ability to convert mechanical stresses to biochemical, bioelectrical, or morphological changes. The cell is thus a mechanical structure with the ability to probe external forces, detect internal mechanics of substructures, and generate responsive and active forces [1]. Section 10.1 cursorily introduces the basic structure of the cell, highlighting key cellular components that are responsible for its mechanical properties and responsiveness.

Maintenance of cellular structures and appropriate cellular responses to external stresses largely depend on the deformability of the cells; the ability to survive the mechanical stress of motility or invasion without rupturing. This is investigated through the elasticity of the whole cell, which in turn informs on its developmental state and pathophysiology. Changes in cell elasticity infer on diseases, which can clinically manifest as a loss in function or change in the physical state of the organ or tissue. The clinical

Viscoelasticity and Collective Cell Migration.
DOI: https://doi.org/10.1016/B978-0-12-820310-1.00010-0

© 2021 Elsevier Inc.
All rights reserved.

relevance of cellular elasticity is thus discussed by giving examples of studies reporting an observed change in elasticity such as the increase in Young's modulus of the zona pellucida of the ovum after fertilization [2], in malaria, asthma, and sickle cell anemia where cellular stiffening was observed [3], or the decrease in elasticity as shown in bladder and cancer cells [4]. Beyond characterizing cell development and function, the significance of tracking cellular elasticity in the pharmaceutical industry is also presented.

Elasticity describes the relationship between stress (force) and strain (deformation). This is the tendency of a material to return to its original shape after being deformed by mechanical stress, graphically presented as a stress–strain curve. The curve/ratio provides information on how much a material can resist forces of stress (stretch). A high elastic modulus implies it takes a lot of force to stretch the material a small amount (the material is then described as being stiff), whereas a low modulus value denotes deformability. Thus it is evident that stiffness is the resistance of a body to deformation upon exertion of an external force and elasticity is a measure of stiffness, reported in the unit of Pascals (Pa). Often, elasticity is reported interchangeably with stiffness. In Section 10.2, methods used to assess cell elasticity, the accompanying physical concepts and current efforts for quantifying a single cell are discussed. Since the average cell dimension is in the micrometer range (50–150 μm typically) [5], imaging techniques need to acquire high spatial resolution planes or volumes to phenotype the whole cell or subcellular structures. The newly introduced technique of optical microelastography, which offers high spatial and temporal resolutions, is presented.

The interpretation of experimental methods used to quantify mechanical properties of cells relies on making assumptions about the cell surface, shape, rheology model, and boundary conditions. The simplest model assumes isotropy and homogeneity of a spherical cell; however, experimental results both from biomechanical and biochemical analyses point toward a more heterogeneous and anisotropic cell, for example, the clustering of integrins versus a more even distribution along the cell membrane [6]. Choosing the right mechanical model is increasingly becoming a key milestone in developing robust methods and more accurate analysis tools for single-cell elastography. However not all tools rely on model analysis, for example, wave-based elastography, which directly characterizes the propagation of a wave through the cell to assess its mechanical property. Consequently, Section 10.3 explores the necessity of and considerations in rheological modeling of a single cell. These computational models can provide more accurate interpretation of experimental results, offering simulation analysis for comparison.

Imaging cellular elasticity has made great strides over the past few decades; the chapter concludes with exploring some miscellaneous techniques that aim to provide wholesome and definitive tools to capture cellular biomechanics. Among the recent trends are assessing both viscosity and elasticity, and providing space and time resolutions to capture dynamic processes of subcellular structures. Assessment of both viscosity and elasticity is necessary because cells are viscoelastic; that is, they exhibit both viscous and elastic properties as a natural consequence of their composition, made of semi-solid organelles, the cytoskeleton, and the nucleus suspended in a fluid cytoplasm. Viscosity is described by the time lag between stress and strain, or the opposition to a movement to maintain a static position when a force is applied. Cells will flow like a fluid and have the ability to recover their shape when the deforming stress is withdrawn. It is thus necessary to develop wholesome and definitive tools that would also quantify the viscosity. Accuracy in such measurements is limited by the reliance on verifying experimental results through computational modeling. Modeling techniques involve gross approximations based on assumptions. To optimize results in cellular elastography, model-independent methods have been suggested to the community. Moreover, the applicability of such techniques to clinical applications depends on their efficiency in processing cells. High-throughput techniques are of interest, and imaging methods used in single-cell assessment are being adapted to increase processing rates. The ability to process millions of cells in a single biological sample should propel elastography to more accurate results as it reduces the incubation time in buffer solutions or media. The ability to provide micrometer-based spatial resolution and millisecond-based temporal resolution could also revolutionize the field by giving access to dynamic changes in biomechanics associated with biological processes.

The walkthrough in this chapter purposes to provide a basis for the unfamiliar reader to understand the basic cell structures responsible for its mechanical properties, available techniques for quantifying single-cell elasticity as well as considerations in choosing a measurement method. The current and future interests of biorheologists, as well as clinical relevance are discussed.

10.2 Cell structure: key architectural players in elasticity

Body parts are a group of organs (bones, muscles, and vessels) that are constructed by different tissues. The tissues are comprised of grouped cells held together by the ECM. The cell is the basic unit of life, which consists of the nucleus, cytoplasm, and membrane. This hierarchical nature of the living body suggests that deformation or mechanical stress to body parts is translated to structural rearrangements of the cell thus potentially affecting its function. Dynamic changes in the architecture and molecular composition of a cell during function, dysfunction or external attack will consequent in changes in mechanical properties of the cell. These mechanical changes on the cytoplasm, membrane, or nucleus can be predictive of developmental failure or markers of healthy versus diseased cells. This section cursorily highlights the key architectural players that modulate the response to mechanical forces and pathway by which mechanical stresses are transmitted.

10.2.1 Cell membrane

The cell membrane is a double-layer of a complex of phospholipids, cholesterol, and proteins embedded with channels that make it semi-permeable. It plays two major roles: (1) provides structural integrity by creating a boundary between the materials inside and outside the cell, and (2) contains passage tunnels for channeling biomolecules into and out of the cell crucial for its homeostasis [7]. The permeability of the membrane as well as its rigidity determine the cell shape and appropriate cellular filtering of biomolecules.

Physical properties of the membrane have been of interest for decades, propelled by elasticity theories [8–10], that highlight the role of membrane elasticity in cell functions like adhesion, motility, cell division, wound healing, and intracellular trafficking. Here, we briefly discuss key structural organization of membrane proteins that contribute to its mechanical properties during normal functioning. The cell membrane is the surface upon which cells adhere to the ECM. Acting as a first point of contact, the flexibility of the ECM regulates receptor adaptability; if the ECM is flexible, rapid deformations are sensed while sustained stresses are dissipated before they reach the cell [11]. Mechanical stresses transmitted to individual cells are distributed via their adhesion to the ECM.

Physiologically, adhesion is crucial in understanding how bacteria, parasites, and viruses interact with a cell. Furthermore, adhesive properties of individual cells determine the cell shape, the structural integrity of tissues, the communication through adhesive junctions, and cell migration [11–14]. The sites of adhesion are provided by cell surface receptors called integrins, which are embedded in the cell membrane where they are activated and participate in binding to the ECM and in cell–cell adhesion [15–19]. The cluster of integrins on the membrane receives the mechanical signal from the ECM and transmits it across the membrane and to the cytoskeleton via a link to actin filaments [20,21].

Both actin filaments and integrins, which are crucial for cell mechanics, are anchored in the membrane and provide a pathway into the cytoskeletal (CSK), defining the cell membrane as a heterogeneous structure [20,22–24]. Actin structures are associated with the membrane in the form of branched and unbranched filaments that regulate protrusion when cells adhere and crawl on a substrate during cell spreading, as well as the ability of the cell to pull itself forward [25,26]. For example, during cell migration, protrusive and contractile forces required for the cell to push and squeeze depend on the rearrangement of actin filaments into subcellular structures on the membrane [27]. Additionally, actin filaments contribute to this motion by forming a crosslink permeated by myosin motors that are essential in cortex regeneration [26]. Moreover, the connection of the membrane to the CSK provides the resistance of the membrane and balances its tension through dynamic mechanical changes [28,29].

10.2.2 Cytoplasm

Within the cytoplasm is the CSK; this is a network of protein fibers that include actin filaments and microtubules, which support the cell shape as well as anchor organelles in a viscous fluid suspension called the cytosol. Mechanical strength of the cell majorly depends on actin filaments that have been shown to dominate in modulating cellular elasticity and by extensional cellular morphology [30–33]. Tensional forces are generated in the cytoplasm as actomyosin slides in their CSK. As for the microtubules, their biomechanical effects on the cell are secondary in that their interaction with actin filaments resists and balances inward directed tensional forces [29,30]. Moreover, such tensional forces are balanced by CSK fibers from individual cells, which are interconnected and through adhesion to the ECM reinforce the mechanical strength of the tissue. CSK forces play an integral role in cell motility by housing and positioning motor proteins crucial in transporting information between the extracellular environment and the nucleus [14]. The rearrangements of actin filaments also mitigate the organization of organelles and corresponding molecules depending on the needs of the cell.

10.2.3 Nucleus

For the eukaryotic cell, the defining feature and largest organelle is the nucleus. It acts as the functional epicenter of the cell containing the genetic material organized as DNA molecules and nucleoproteins to form chromosomes. The nucleus is isolated from the rest of the organelles by a double membrane that is selectively permeable and structurally supported by the nucleoskeleton. Through the LINC (linker of the nucleoskeleton and cytoskeleton) complexes, forces are transmitted between the cytoskeleton and the nucleus. The physical connection between the CSK and nucleoskeletal has been hypothesized as crucial in intracellular nuclear movement and positioning, in CSK organization and cell migration, as well as in triggering force induced changes in nuclear structures. Albeit in its infancy, research in nucleo-CSK coupling and the role of the proteins in the LINC complex is deemed essential in elucidating how the nucleus processes mechanical forces [34] and in understanding the effects on gene expression.

From the above review, it can be concluded that the effect of mechanical stresses on the cellular functionality and shape depends on the mechanical properties of the ECM, the organization of membrane proteins and CSK filaments, cytoplasmic tensional forces, and the cyto-nucleoskeletal coupling. Proper distribution and transmission of mechanical forces and the ability of the cell to perform its function while maintaining structural integrity; that is, without shearing or breaking, is the basis of cellular elasticity.

10.2.4 Clinical relevance of cellular elasticity

Correct physiology and appropriate mechanotransduction—how cells sense and transform mechanical signals into biochemical processes, depend on the elasticity of the cell components. Dysfunction at any point in cellular mechanics may consequent in cell, tissue, and organ pathophysiology or developmental abnormalities resulting in diseases spanning a wide range of fields in health [35–39]. A few examples of elasticity changes manifested clinically in diseases include decreased lung elasticity in emphysema [40], breast and bladder cancer cells [41,42], narrowing of airways in asthma [43], enhanced rigidity and adhesion of red cells to the endothelium in malaria and sickle cell disease [44,45], increased stiffness of brain cells and tissues in Alexander disease [46], increased stiffness in ECM of the lung in idiopathic pulmonary fibrosis [47], reduced stiffness in emphysematous lung tissues and chronic obstructive pulmonary disease [48,49], arterial stiffening in hypertension [50], reduced elasticity in gastrointestinal cancer, malaria, and human breast epithelial cancerous cells [51,52], increased stiffness in myofibrillar myopathies [53], and body weight loads and urine pressure causing cell necrosis in diabetic foot ulcers and kidney disorders [28].

The correlation of cellular elasticity with morphology has gained momentum in the pharmaceutical industry with calls for the creation of a unique area termed as "mechanopharmacology" [54]. This would focus on the consideration of cellular mechanics in identifying drug targets, particularly drug action on the cell [55,56]. Knowledge of cellular biomechanics has two major contributions to pharmaceutical developments: (1) development of pharmacological agents that are biomechanically similar to the target organ and tissue, mainly the creation of substrates that span the known pathophysiological range of cells in which to develop drugs [57], and (2) identification of cellular stiffness as a biomarker of therapeutic activity. Studies that have exploited stiffness as a biomarker include but are not limited to: antimitotic microtubule targeting agents that have been correlated to corrected whole-cell stiffness on cancer cells [58]; reduction of inflammation of endothelial cells by the simvastatin drug, as illustrated by elasticity changes [56]; and observed increase in cell membrane permeability (reduced elasticity modulus) by glycyrrhizin, in the development of drug delivery systems [59].

Moreover, investigation into the elasticity of pathogens is instrumental in elucidating pathogen–host interaction, particularly pathogen adherence in drug screening. The elastic properties of the bonds between the pathogen and host have been shown to be responsible for robust adhesion and cooperation [60–65]. Such mechanical properties have been used to investigate adhesion of *Borrelia burgdorferi* in Lyme disease [66], binding of the Ebola virus to the host cell membrane [67], the membrane properties of *Escherichia coli* [68], and the effect of membrane stiffening of red blood cells on deformations resulting from adhesion of malaria parasites [69].

Cellular elasticity can also be used to phenotype mutations of said pathogens and potential immune evasion. In *Candida albicans*, a common human fungal pathogen, mutations of the wild type have been reported to have decreased cell wall elasticity [70], whereas wild type 042pet *E. coli* is reported to be more rigid that the mutant 042aap [71].

Pointedly, most of the clinical manifestations of diseases are related to changes in tissues and by extension of cellular mechanics [35,72]. Scientists have responded to this by focusing studies beyond genetic testing and to physical phenotyping of tissues and cells, with hopes to elucidate the effects of mechanical stresses on biological functions. To this end, molecular biologists now focus on the pathways in which mechanical forces are converted to biochemical signals in the field of mechanotransduction, which is the process by which cells convert mechanical stimuli to biochemical signals [21,34,35,73,74]. On the other hand, physicists and engineers apply rheological methods (the science of deformations and flow) to understand cellular mechanics.

Rheology primary deals with the relationships between stresses and deformations and has been applied over different industries from chemical processing (plastics, paints, and lubricants) to geological seismology and most notably biotechnology (cellular and biomaterials) [75]. A wide array of techniques have been developed with length scales to probe cellular elasticity, viscosity, and viscoelasticity. By inducing external mechanical stresses, the response from the cell can be tracked and used to phenotype its properties, development, and pathophysiology. Albeit not all novel technologies as atomic force microscopy (AFM) or optical tweezers have been around for decades, recent developments to push the spatiotemporal scales would potentially enable the capture of dynamic processes in addition to biomechanical phenotypes. Advancements in such techniques are presented more thoroughly in the following section.

10.3 Estimation of cell elasticity

Viscoelasticity is a fundamental property to better understand biological cells. This parameter is indeed related to the cell anatomy, functionality, and pathological state. Due to its importance, various techniques have been developed to estimate it.

10.3.1 Cellular deformation

Most widespread techniques to estimate cell viscoelasticity are based on cell deformation. Cells can be deformed in many ways, including micropipettes or microplates [76], microfluidic deformation [77,78], magnetic bead twisting [79], and tweezers or stretchers [80]. Micropipettes, microplates, and microfluidic tubes can deform the cell by various ways, notably aspiration, squeezing, tubular constrains, etc. More information on optical, acoustic, and magnetic tweezers is provided later in this chapter. Active or passive cell deformation can be observed from optical images under a microscope. Global elasticity (or whole-cell elasticity) can then be estimated from the applied force intensity and the observed deformation. Viscosity can also be deduced by observing deformation along time.

However, mapping both viscosity and elasticity is more difficult because the local deformation depends strongly on the internal distribution of stress, which is unknown. Scientists can use different models to estimate this distribution, but the assumptions behind the model have a strong influence on the final estimation. As an illustration, mouse oocyte zona pellucida elasticity was measured in two independent experiments [81,82]. The first team found a value of 3–14 (± 2) kPa depending on the model, and the second group reported a value of 42.2 ± 2 kPa. Hence, the results strongly depend on the model and images are hardly quantitative [83] but offer approximations. Despite this drawback, cell deformation is widely used nowadays, thanks to its simplicity and adaptability to different setups. Also, spatial and temporal resolution can be excellent, as they mainly depend on the camera pixel resolution and frame rate.

10.3.2 Cellular deformation using tweezers

An important cellular deformation technique lies in the use of optical tweezers or stretchers [84–86]. It is based on the difference in refractive index between different parts of the sample (or with the surroundings). Due to this difference in optical property, a focused laser beam can trap a part of the cell and move it. One can then deform the whole cell to estimate its global elasticity [85]. However, it is rarely used to map elasticity from local deformations [86], as it needs an appropriate modeling of the cell mechanical behavior (similarly to the cell deformation with micropipettes); and it is complicated to trap only a point of the cell, requiring to add external optical beads (making the technique very similar to active microrheology, described later). The technique presents nevertheless the advantage to be contactless and quite easy to implement. It is often used to measure red blood cells global elasticity [87–89]. Cell tweezers were also developed using acoustic [87,88] and magnetic fields [89,90].

10.3.3 Atomic force microscopy

AFM has widely been used to map cell elasticity [91–93] and has become with time one of the standard to assess cell viscoelasticity. With this technique, the cell is poked with a small cantilever. Cantilever displacement is measured through the deviation of a laser beam. Measurements are done point by point, allowing to reach a submicrometric resolution. Viscoelasticity can then be deduced from the temporal response of the cantilever penetration at each point of the medium. Similarly to cell deformation techniques, AFM needs an appropriate physical modeling, as even if the applied force can be precisely measured, the stress distribution in the sample is unknown. As measurements highly depend on the chosen model, AFM requires a precise calibration of the cantilever shape: change in shape due to probe aging, in particular, can have an important impact. Finally, due to the mechanical measurement point by point, acquisitions are rather slow, taking typically at least a few minutes to achieve a reasonable number of data points. One must be careful that no biological process impacting cell viscoelasticity occurs during the acquisition time—this is not always negligible: for example, a study using a micropipette indentation showed that mouse oocyte elasticity was decreasing by a factor of two in less than 10 seconds during probing [94]. The long period of acquisition with AFM also requires the cell to be fixed to the support, a process which can alter cell characteristics. Also, although some models allow to measure viscoelasticity in the bulk, this technique essentially makes surface measurements [95] (Fig. 10.1).

10.3.4 Microrheology

Microrheology is a technique initially developed to assess viscoelastic properties of soft matter [96,97]. This technique uses micrometer sized spheres as particle probes. Each particle is then individually tracked over time—typically for a few minutes. We usually distinguish "passive microrheology," where particles are moving due to Brownian noise, and "active microrheology," where particles are moved by an external force (magnetic field, optical tweezers, etc.). Note that "active microrheology" is

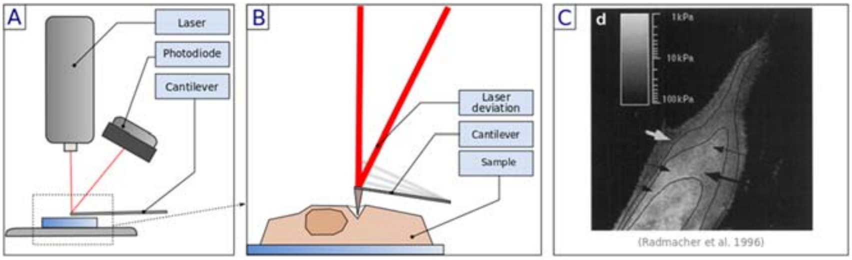

Figure 10.1 (A) and (B) Schematic of an AFM experiment. A cantilever is poking a cell attached to a substrate. This deviates a laser detected by a photodiode. (C) The deviation behavior gives information on the cell elasticity at each point. *AFM*, atomic force microscopy. *From M. Radmacher, M. Fritz, C.M. Kacher, J.P. Cleveland, P.K. Hansma, Measuring the viscoelastic properties of human platelets with the atomic force microscope, Biophys. J. 70 (1996) 556–567.*

sometimes named from the external force type: for example, "magnetic twisting cytometry." In magnetic twisting cytometry (MTC), microbeads are allowed to bind to cell surfaces for 10–15 minutes. Introducing a strong magnetic field (1000G for 10 microseconds) allows magnetization and alignment of magnetic moments of the cell bound beads. Mechanical stress is then applied using a weaker twisting magnetic field that is perpendicular to the original magnetic field. Finally, measurement of the average bead rotation induced by the twisting magnetic field allows the estimation of mechanical properties of the cell [79,98,99].

The particle density has to remain low to facilitate tracking, and more importantly, to limit particle interactions due to the Van der Waals force or other forces that would influence particle displacement. Knowing the physical force which makes them to move and the mean square displacement of each particle allows the estimation of both elasticity and viscosity of the sample at the particle locations. Hence, microrheology cannot provide detailed maps of a sample viscoelasticity, but rather measurements at discrete particle locations.

Nonetheless, microrheology has been applied to assess mechanical properties of biological cells [100]. Scientists have been able to estimate both elasticity and viscosity in different zones of the cells, such as the interphase, nucleus, and cytoplasm [101]. However, applying this technique to biological samples makes the assumption that the particle displacement is only due to physical processes. This assumption can be invalid for active cells and/or long measurement times, making this technique less reliable. Another drawback lies in the invasive nature of the method: particles have to be injected inside the cell for tracking purpose without impacting its functionality (Fig. 10.2).

10.3.5 Brillouin scattering microscopy

Brillouin scattering microscopy has been introduced and further developed recently to estimate cell elasticity [102,103]. This technique entails transmitting a laser beam in the studied cell. Internal mechanical waves inside the cell shift the laser frequency. Measurement of this shift allows to estimate bulk elasticity modulus at the laser beam location. By moving the laser beam point by point provides 2D and even 3D measurements. In 2015 Scarcelli et al. [102] showed that the bulk modulus varies proportionally with the Young modulus in NIH 3T3 cells with various concentration of sucrose. This might not be true for all samples, as even in a homogeneous isotropic linear elastic material, the physical relationship between these two magnitudes involves a third parameter (Poisson's ratio). This method, as with most microrheology technologies, is rather sample dependent: for example, in hydrated materials, water content dominates Brillouin spectroscopy measurements instead of stiffness [104]. However, although it can reach a good spatial resolution ($0.5 \times 0.5 \times 2\ \mu m^3$ in Scarcelli et al.), the point-by-point measurement makes the acquisition of a large number of points rather slow, typically a few minutes (Fig. 10.3).

10.3.6 Microelastography

Shear wave elastography is a technique developed a few decades ago to map organ viscoelasticity, through ultrasound imaging [105,106] or magnetic resonance imaging [107]. It has been successfully applied in many

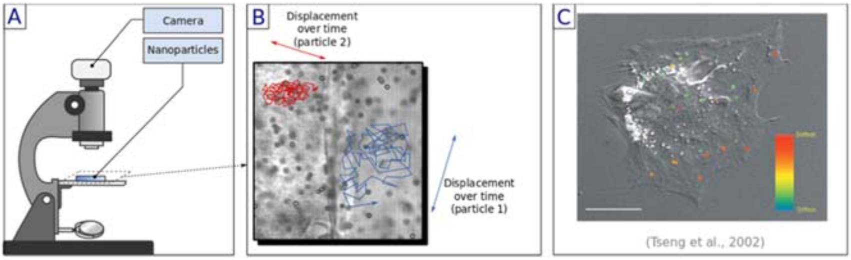
A
Camera
Nanoparticles
B
Displacement over time (particle 2)
Displacement over time (particle 1)
C
(Tseng et al., 2002)

Figure 10.2 (A) and (B) Schematic of a microrheology experiment. Particles are injected in the sample. A camera tracks the particle along time. (C) The mean square displacement of particles allow to evaluate local viscoelasticity. *From Y. Tseng, T.P. Kole, D. Wirtz, Micromechanical mapping of live cells by multiple-particle-tracking microrheology, Biophys. J. 83 (2002) 3162–3176.*

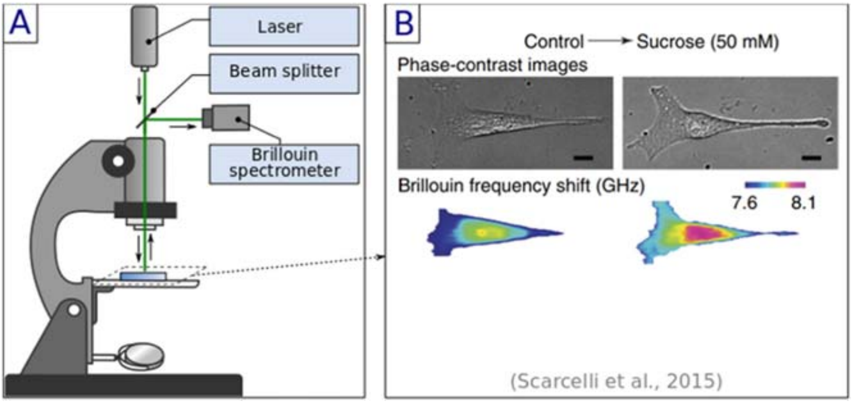

Figure 10.3 (A) Schematic of a Brillouin spectroscopy experiment. A laser beam is emitted on the sample. Longitudinal waves inside the cell shift the laser frequency. A Brillouin scattering then measures the frequency shift, related to the local longitudinal elasticity modulus. (B) A map of the Brillouin frequency shift can be produced with a high spatial resolution. *From G. Scarcelli, W.J. Polacheck, H.T. Nia, K. Patel, A.J. Grodzinsky, R.D. Kamm, et al., Noncontact three-dimensional mapping of intracellular hydromechanical properties by Brillouin microscopy, Nat. Methods, 12 (2015) 1132.*

organs, including the liver [108], breast [109], and the thyroid [110]. This technique is based on tracking of a type of mechanical wave, the shear wave, in the studied sample. As the shear wave speed is related to the sample elasticity under certain assumptions, one can map elasticity by measuring the speed of the shear wave everywhere in the sample. Besides, shear wave amplitude also decreases with viscosity, so this parameter can be also estimated from the shear wave attenuation over distance [111]. Concretely, in shear wave elastography, a time-lapse of the sample is imaged, usually with ultrasound or magnetic resonance imaging. A shear wave is induced in the sample, through a mechanical or acoustical vibration, and images are captured as the wave propagates through the sample. The displacement between images is calculated with a tracking algorithm. Elasticity and viscosity are then mapped in the sample from the displacement propagation as shear waves.

This technique has been recently applied at the cellular scale [112], by achieving three main milestones:

1. the generation of shear waves at high frequency (15 kHz), at least 10–300 times higher than the usual shear wave frequency used in elastography;

2. the high-speed detection of the waves; indeed, in soft matters, shear waves usually propagate at a speed of a few meters per second, so tracking the shear waves in a sample of a few tens of micrometer requires an imaging frequency higher than 100,000 kHz. In the reported experiments of Grasland-Mongrain et al., a 200,000 frames per second (fps) optical camera was used; and
3. the use of correlation-based techniques to calculate displacement propagation; as the shear wave front was not well defined in reported experiments, a robust 2D optical-flow-based speckle tracking method had to be used.

With these three challenges resolved, the technique could be used to map the elasticity of $\approx 80\,\mu\text{m}$ diameter mouse oocytes. The authors reported a spatial resolution of about 10 μm, for a measurement acquired in less than 1 microseconds. Despite this relatively low spatial resolution, the measurement speed is an important advantage to follow dynamic cellular processes. Also, the time resolution avoids artefacts due to changes in cell biomechanics during measurements. Scientists are currently trying to improve the spatial resolution by using different types of shear waves and by improving elasticity estimation algorithms. Theoretically, the spatial resolution limit should be the one of optics; so it is anticipated that a submicrometer resolution could be achieved. One important point of the technique is the absence of viscoelastic model required to reconstruct cell biomechanics, contrary to cell deformation techniques. But this goes with a difficulty: cell elastography primarily provides wave speed information, which can be related to cell elasticity assuming some a priori on shear wave propagation and cell property. Additionally, the method has not yet been developed to measure cell viscosity (Fig. 10.4).

10.3.7 Summary

In summary, depending on the application, estimating the viscoelasticity of a whole cell in a few locations can be sufficient, without the need to locally map this parameter with a good spatial resolution. Also, some techniques are able to estimate both elasticity and viscosity of the sample, whereas some only provide one of these parameters, or a combination. A single method is currently able to map cell elasticity at a temporal resolution on the order of a millisecond. The choice of the measurement method can vary depending on the results of interest. The table below offers a summary of discussed methods (Table 10.1).

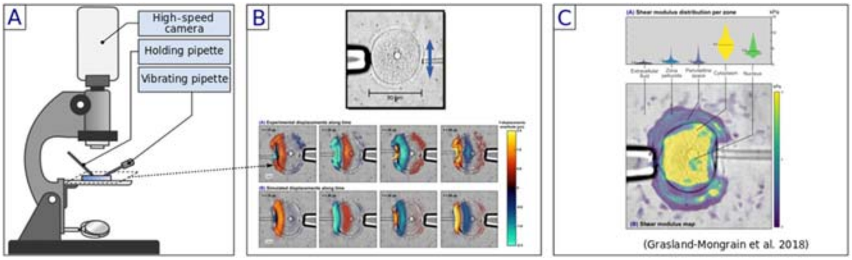

Figure 10.4 (A) Schematic of a microelastography experiment. A pipette is vibrating the sample. The vibration propagation is observed by a high-speed camera. (B) A computer algorithm is then estimating the local shear wave speed, related to the cell elasticity. (C) Map of the cell elasticity. *From P. Grasland-Mongrain, et al., Ultrafast imaging of cell elasticity with optical microelastography, Proc. Natl Acad. Sci. U. S. A. 115 (2018) 861–866.*

Table 10.1 State-of-the-art rheology technologies to assess cell viscoelasticity and description of performance.

	Setup simplicity and price	**Spatial resolution**	**Temporal resolution**	**Measured physical parameters**
Cell deformation [76,79,82]	++	<μm	≈second	Deformation
Optical tweezer [85,86,113]	+	<μm	≈second	Deformation
Atomic force microscopy [91–93]	−	≈μm	≈minute	Cantilever deviation
Nanoparticles tracking [114]	+	>10 μm (no	mapping possible)	>minute
Particle mean square displacement				
Brillouin scattering [102,103]	−	≈μm	≈second	Brillouin frequency shift (related to the longitudinal modulus)
Microelastography [112]	−	>10 μm	≈millisecond	Shear wave speed

10.4 Rheological modeling of a single cell

This section is highlighting some of the models applied for the interpretation of experimental data used to quantify cellular elasticity. Modeling of living cells attempts to quantify mechanical properties and responses when perturbed by an external load or stress. There are principally two schools of thought on the physical distribution of forces by cells: the micro/nano-structural approach and continuum models. Structural approaches consider discreet load-bearing elements, with the cytoskeleton as the main component. Continuum models, on the other hand, consider load-bearing elements that are infinitesimally small relative to the size of the cell. Biomedical models allow for the quantification of experimental data by making assumptions on the cell surface and shape, with the simplest model assuming homogeneity and isotropic distribution of mechanical stresses.

Noteworthy, is that although some general models have been developed, there is not a "one ring to rule them all" universal model to quantify mechanical properties of living cells due to their dynamic nature and ability to adjust to different microenvironments. Moreover, rheological techniques use different types of forces, magnitudes, and loading rates that are eliciting different responses from the cells [115,116]. Rheologists should thus choose a model that appropriately fits testing conditions, is physiologically relevant, and is descriptive of specific cells. After briefly introducing basic principles of each model, recent insights such models have provided are highlighted in the context of cellular elastography.

10.4.1 Structure-based models

10.4.1.1 Tensegrity model

Micro/nano-structural approaches deem the cytoskeleton as the main structural component with the widely accepted composition of microfilaments, microtubules, and intermediate filaments. The organization and association of this meshwork influences cellular tension and alternations responsible for cell shape and movement. The complexity of this structure in its most basic form is architecturally modeled as six wooden bars that are not in contact but are connected to a series of 24 elastic strings which hold up the rigid bars in an approximate sphere. The integrity of this structure is observed when a force is exerted from above flattening it out or anchored at the bottom spreading it out, without breaking. When compressional forces are released, the structure spontaneously reverts to its original shape, whereas the rigidity of wooden bars remains unchanged. The reliance of shape integrity on internal tension gave this model its name—tensegrity for tensional integrity [117–119].

This model, adapted from construction architecture, is applied to biological cells by making a number of assumptions [118,120–123]. These include: (1) mechanical load of cells are transferred across points where they anchor to their support system, that is the ECM or to other cells; (2) the cytoskeleton is responsible for the internal tension of a cell; (3) at molecular scales, local force interactions are dominant to gravitational effects, which means that the gravity is negligible; and (4) a compressible nucleus allows the extension of tensegrity to the nucleoskeletal, that is the whole cell can adhere to the ECM or to other cells and stretch in cell spreading without breaking or shearing.

Using this 30 structure model, an expression for the elasticity is derived based on a coarse-grain procedure. The working principle of the derivation is that external forces E on the model are equal to the strain energy and follow the relationship presented in the equation below [124]:

$$E \approx \frac{\sigma_c^0 \varphi_c}{3} \approx \frac{\sigma_s^0 \varphi_s}{3}. \tag{10.1}$$

The above equation can be applied to experimentally generate upper and lower bounds of cellular elasticity, where σ_c^0 is the initial tensile stress of the strings, φ_c is the relative density of the strings, σ_s^0 is the initial compression stress in the wooden struts, and φ_s is the relative density of the wooden struts. This is achieved by identifying the tensile strings with the CSK actin filaments and the wooden struts with the microtubules [125,126].

Years of experimental proof have seen tensegrity been adapted in different studies, especially for investigating CSK mechanics in adherent cells and in determining the structural origin of cellular viscoelasticity. The tensegrity model has supported experimental efforts in characterizing the response of CSK elements on global CSK behavior [127], dynamics of cell reorientation in collective cell alignment and movement [128], and quantification of cellular elasticity providing strong evidence that the CSK is the primary determinant of the cell elastic response [125,126,129,130] (Fig. 10.5).

Despite the ability of the tensegrity model to accurately predict elastic characteristics of cells, it has a few limitations that include: failure to

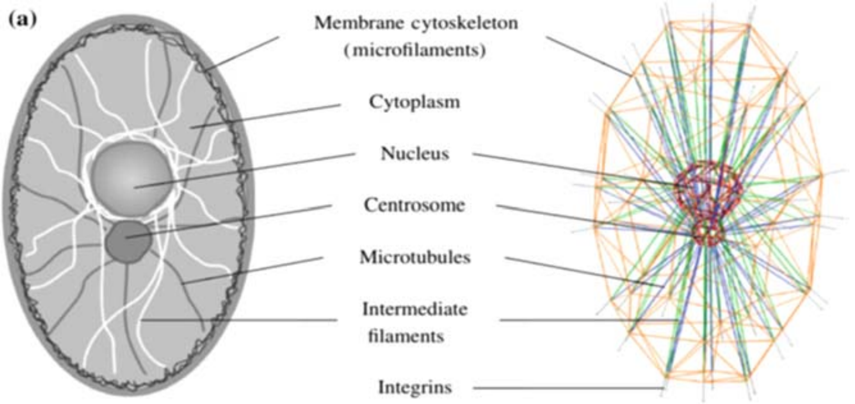

Figure 10.5 (A) Tensegrity model of the cell, with the comparator of the cell structure to the model, highlighting key structural elements. *From L. Zhang, X. Feng, S. Li, Review and perspective on soft matter modeling in cellular mechanobiology: cell contact, adhesion, mechanosensing, and motility, Acta Mech. 228 (2017) 4095–4122.*

consider effects from thermal and nonthermal fluctuations, effects from the nuclear membrane and the fluid-like cytosol and compressibility of the microtubules, which are modeled as rigid struts. In the simplicity of the tensegrity model lies its elegance and flaws in characterizing complex hierarchal biological structures. Nonetheless, efforts are in place to develop more robust and multiscale tensegrity models incorporating considerations such as relaxing the rigidity of the struts, and introducing compressibility and hyperelasticity of the bars thereby accounting for nonlinear responses [131,132]. Needs are also to consider models that incorporate the nucleoskeletal capturing the hierarchical cell [122].

10.4.1.2 Percolation model

A model adapted from the mathematics and material science fields, namely the percolation theory, describes the random organization of elastic clusters. The emphasis of this model is in the connectivity of basic units, which are essential in information transfer [133]. Above a critical concentration of subunits or a percolation threshold, the structure develops elastic properties capable of response to mechanical stimuli. This threshold highly depends on the random geometry of the arrangement giving the structure great flexibility in assemblies, consequently the elasticity of the structure is dynamic [116,134]. The constituent subunits can assume any shape and randomly connect, thus changing global elasticity while adjusting to the environment. Biologically, interconnected networks are plenty within the cell inclusive of the nucleoskeletal filaments, CSK, or ECM. This model views the CSK as an entangled random mesh of network forming macromolecules. Applying the percolation model to the assembly of such networks explains morphogenic motions that are driven by the matrix. That is, locally assembled interconnected filaments and microtubules are dynamic and constantly rearranging while maintaining a global elasticity.

The percolation model does not compete with the tensegrity model, on the contrary the two can be thought of as complementary. As discussed in Ref. [133], tensegrity structures could develop from assembly of percolation structures. Moreover, there is the shared characteristic of interconnected ness and dynamic subunits contributing to a global sensitivity that allows uninterrupted propagation of stimuli. Unfortunately, this model has remained highly conceptual with limited quantitative results or correlation to elasticity [135]. Efforts to quantify elasticity based on a percolation, percolation-like model, or composite model include: calculation of the shear modulus of membrane skeleton based on a random incomplete lattice of spectrin tetramers [134], use of a random graph model of the spectrin CSK to investigate changes in red blood cells [136], and modeling skin lattice based on percolation to investigate tissue aging, which is correlated to elasticity loss [137].

10.4.2 Continuum-based models

Instead of focusing on particular constitutive structures as the main determinant of elasticity, continuum models focus on the continuous distribution of forces and strains within the whole cell, thus providing less details [115]. These models are, however, easier and direct in extracting mechanical properties and correlating them with experimental observations. The simplest model of the cell assumes isotropy and homogeneity; however, experimental results pointing to a more viscous nucleus compared to the cytoplasm have redirected model analysis to more robust options that capture heterogeneity, anisotropy, and viscoelasticity. Below such models are discussed.

10.4.2.1 Liquid drop models/cortical shell liquid models

These models are based on the assumption that cells behave like a liquid drop. That is, they adapt a spherical shape when suspended, deform continuously as response to suction pressure into a micropipette acquiring a smaller diameter, and steadily recover the initial spherical shape upon release [138]. These models were first developed for the rheology of neutrophils in micropipette aspiration. Among these models are the simple and compound Newtonian liquid drop, shear thinning liquid drop model, and the Maxwell liquid drop model. The first three are satisfactorily suited for modeling large deformations. For the simple Newtonian liquid drop model, the cell is assumed to be a homogenous viscous liquid with a cell cortex that is anisotropic and with statistic tension. For example, leukocytes adopt a spherical liquid drop shape when suspended [138]. The constitutive equation of this model approximates the cell membrane and its cytoskeleton as a liquid cortical layer with negligible viscosity and a constant surface tension until an expansion limit is achieved [76,139,140]. Such studies have revealed the overall elasticity and viscosity to vary continuously with the degree of deformation [141].

The compound Newtonian model takes into account the nonhomogeneity of the interior of the cell; with a nucleus that is stiffer and more viscous than the cytoplasm [141–143]. Eukaryotic cells that are composed of a cell membrane, a cytoplasm, and a nucleus can be modeled with this approach. The model divides the cell into a three layered structure; the ectoplasm which is under persistent tension, the endoplasm as the softest region which is fluid-like, and the core layer composed of a condensed nucleus. For the structurally heterogeneous cell to behave as the simple Newtonian model, a few considerations should be accounted for: the time-scales of the cytoplasm and nucleus as well as the initial deformation ratio of the nucleus to the cytoplasmic shell should be comparable [144–146]. Time-dependent behavior of passive neutrophils due to large deformations can be explained by the compound liquid drop model in this manner [145]. There could be an infinite number of possibilities to fit a particular rheological model to study cell recovery depending upon the cell type and the experimental setup, meaning that only one kind of experiments cannot sufficiently identify all viscoelastic properties that are concerned. Among the success of this method is that in its limitations it is understood that dealing with the cell as a whole is inadequate when studying heterogeneous structures and a more accurate model would deal with the structures (cortex, cytoplasm, and nucleus) individually [115,147]. Like Newtonian models, shear thinning is based on micropipette aspiration. The underlying principle relies on the apparent viscosity of the cytoplasm that decreases with increasing mean shear rate, that is, the aspiration pressure. In the Newtonian liquid model, the aspiration speed is constant under constant aspiration pressure, however, the observed acceleration right before the whole cell is sucked in takes the form of a power law [148]. Combined with a finite-element-model, the shear thinning explanation is promising as it performs well in different experimental conditions capturing the complex cellular geometry during aspiration and other nonlinear relationships [115,149,150]. Shear thinning is successful in providing a comprehensive picture of cells during micropipette aspiration, however, other measurements with small scale dynamics do not exhibit shear thinning, limiting the above models to modeling larger deformations in cells.

To account for short-time smaller deformations, the Maxwell model which assumes a prestressed cortical shell containing a Maxwell fluid is better suited to explain the initial rapid entry during the micropipette aspiration of the cell [151]. Here, the cortical shell represents the near-surface actin layer of the cell, whereas the Maxwell fluid constitutes average mechanical properties of the cytoplasm with the main difference being that a Maxwell model contains an elastic component. This model was first utilized to study the recovery behavior of passive leukocytes in micropipette aspiration under small deformations [151]. Later, this model was also extended for large leukocyte deformations using a finite element method analysis to show that the Maxwell liquid model could not accurately describe the experimental data without allowing elasticity and viscosity values of the cytoplasm to increase computationally as the cell gets sucked into the pipette [141,152]. The constitutive equation is as below [151], where a dashpot and spring in series capture mechanical properties in k as an elastic constant and μ as a viscous constant. The parameter τ_{ij} is the deviatoric stress constant, $\dot{\tau}_{ij}$ is its spatial derivative, and $\dot{\gamma}_{ij}$ is the engineering strain constant [153]. Noteworthy is that the Maxwell model degenerates into a Newtonian model as the elastic constant k approaches infinity, implying that as the cell is being aspirated it transitions from a Maxwell to a Newtonian fluid with increasing elasticity and viscosity moduli [115]. This model is given by:

$$\tau_{ij} + \frac{\mu}{k}\dot{\tau}_{ij} = \mu\dot{\gamma}_{ij}. \tag{10.2}$$

Small deformation behavior in cells is fundamentally different than the large deformation of flow. In the above equation, if k approaches to infinity, the Maxwell fluid degenerates into a Newtonian fluid, meaning that the cytoplasm undergoes a transformation from the Maxwell to the Newtonian behavior during micropipette aspiration, with increased elasticity and viscosity moduli. If the cell holding time is very rapid (5–7 seconds), the sausage shape deformed cells can exhibit a rapid initial elastic recovery [141]. However, if cells are to be held for a longer duration, the recovery becomes slower and the Newtonian liquid behavior dominates [145,146]. Perhaps the most significant contribution of the Maxwell model is in identifying cells as viscoelastic.

10.4.2.2 Solid models

Solid models assume that cells are made of one or more homogeneous layers and the incorporated material models may range from incompressible elastic to a viscoelastic solid depending upon experimental conditions. Cells are considered to be in a solid phase and the homogeneity assumption simplifies experimental data analysis as several mechanical parameters vanish from the mathematical equations. In micropipette experiments, endothelial cells and chondrocytes could not flow into the pipette even when the suction pressure was beyond the critical suction pressure, giving it a solid-like behavior [154,155]. Furthermore, nonspherical shapes in such experiments can be attributed to the reassembly of the cytoskeleton elements in response to the shear stress making it behaves like a solid rather than a fluid. Solid models are discussed separately for linear elastic and linear viscoelastic materials in the following subsections.

Linear elastic solid model

In a linear elastic model, cells are assumed to be in a solid phase with homogeneous and elastic properties. This model is a simplification of the viscoelastic solid model in which the time factor is ignored. The elasticity of the cell can then be represented in terms of its shear modulus G. Under the assumption of linear elasticity, the shear modulus is related to the Young's modulus E by the equation $E = 2(1 + \nu)G$, where ν is the Poisson's ratio approximately equal to 0.5 for an incompressible material. Even though such a linear elastic model may not be adequate for describing cell mechanics, it serves as a basis for the viscoelastic solution.

In micropipette aspiration experiments, the radius of the cell is much larger than the radius of the pipette, and so, the cell is approximated as an incompressible elastic half-space. If the applied suction pressure is ΔP, the aspiration length of the cell is L, the radius of the pipette is R_p, and the ratio of the pipette wall thickness to the pipette radius is ϕ_P (ϕ_P = 2.0–2.1 when the ratio is equal to 0.2–1.0), then the shear modulus G can be computed as [154]:

$$G = \frac{\phi_P \Delta P}{2\pi\left(L/R_p\right)}. \tag{10.3}$$

For AFM indentation of adherent cells, if F is the indentation force, θ the indentation angle, and δ is the indentation depth of the AFM tip, then the shear modulus can be computed as [156]:

$$G = \frac{F(1-\nu)\tan\theta}{1.4906\delta^2}. \tag{10.4}$$

The indentation of adherent cells can also be performed using a cytoindenter or a cell poker. For a cell poker with a cylindrical tip whose surface curvature and cell thickness are larger compared with the cylindrical diameter, the linear elastic solution to compute the shear modulus can then be expressed as below, where R_I is the radius of the indenter:

$$G = F\frac{1-\nu}{4R_I}. \tag{10.5}$$

Finally, for MTC experiments [79,98,99], a finite element method can be utilized to achieve an analytical solution [157]. The spherical magnetic field is assumed to be fully adhered to the cell surface, and the bead and the substrate are assumed to be rigid. The expression to compute the shear modulus can be given as:

$$G = \frac{T}{k_s\alpha}\left(\frac{1}{\phi}\right) \text{ or } G = \frac{TR}{k_s\beta}\left(\frac{R}{d}\right), \tag{10.6}$$

where T is the applied torque, k_s is the shape factor for the bead, ϕ is the angular rotation of the bead, R is the radius of the bead, d is the displacement of the bead, and α and β are constants that depend on the cell height and the amount of embedded beads.

Linear elastic models are useful for simplified computations and thus for determining the estimate of the shear modulus. However, cells are often surrounded by fluids such as lipid membrane, which make them exhibit both fluid-like and solid-like properties. Thus linear viscoelastic models are utilized to integrate both of these material phase properties.

Linear viscoelastic solid model

The linear viscoelastic solid model can be considered equivalent to having a Maxwell model in parallel with a spring element. Such a model can be used to study the small-strain deformation of cells, such as human leukocytes in micropipette aspiration experiments. The creep response $L(t)$ for a micropipette experiment can be given by [158]:

$$\frac{L(t)}{R_p} = \frac{\phi_P \Delta P}{2\pi k_1}\left[1 + \frac{k_1}{k_1 + k_2} e^{-\frac{t}{\tau}}\right] H(t), \tag{10.7}$$

where k_1 and k_2 are elastic constants, $H(t)$ is the Heaviside function, and τ is the characteristic creep time given as:

$$\tau = \mu \frac{k_1 + k_2}{k_1 k_2}, \tag{10.8}$$

with μ being the viscous constant. For a cell poker experiment with a cylindrical tip, the response of an adherent cell to a creep indentation $\delta(t)$ is given as [115,159]:

$$\delta(t) = \frac{F}{8R_I k_1}\left[1 + \left(\frac{k_1}{k_1 + k_2} - 1\right) e^{-\frac{t}{\tau}}\right] H(t). \tag{10.9}$$

These linear solid models were first applied for modeling leukocytes. However, leukocytes were found to be more accurately described using liquid drop models. Several anchorage-dependent cells such as endothelial cells, osteoblasts, chondrocytes, and cell nuclei follow standard linear solid models [155]. Both linear elastic and linear viscoelastic models are utilized for cell modeling or for investigating changes to cellular mechanics under different requirements and different conditions. Applications include models that can be utilized to determine properties of different types of cells. These models can also be used to study cellular deformation [160,161].

10.4.2.3 Power law structural damping model

The dynamic behavior of cells is often studied in conditions where they undergo dynamic forces. Generally, MTC and AFM techniques are utilized for conducting dynamic tests on adherent cells, where a low amplitude sinusoidal force signal results in a sinusoidal displacement at the same frequency but exhibiting a phase lag in its steady state. Alcaraz et al. [162] developed a mathematical model for computing the complex shear modulus in an oscillatory AFM experiment by implementing a correction term to account for the contribution of the hydrodynamic drag force that may be significant due to viscous friction. In MTC experiments, the complex shear modulus may be computed from the classical elasticity equations with the condition that a linear viscoelasticity model is valid.

However, in both AFM and MTC experiments, the real part of the complex modulus of cells may depend on the frequency (ranging typically from 10^{-2} to 100 Hz) that can be defined by a weak power law with an exponent between 0.1 and 0.4.

The complex part of the shear modulus also exhibits a power law frequency dependency at low frequencies (<10 Hz); but at higher frequencies, the Newtonian viscous component overcomes it. This behavior was observed in several human cells including bronchial and alveolar epithelial cell lines [162], airway smooth muscle cells, lung epithelial cells, neutrophils, and mouse cells such as embryonic carcinoma cells and pulmonary macrophages [98]. Such nonlinear behavior cannot be accurately determined by spring-dashpot models (Maxwell, Newtonian, linear models), since the spring-dashpot system may always overestimate the exponent of the power law. Thus a power law structural damping model based on experimental findings was proposed to observe rheological behavior of adherent cells [163]. According to this empirical model, the complex shear modulus of adherent cells can be expressed as:

$$G^*(\omega) = G' + iG'' = G_0\left(\frac{\omega}{\omega_0}\right)^{\alpha}(1 + i\eta)\Gamma(1-\alpha)\cos\frac{\pi\alpha}{2} + i\omega\mu. \tag{10.10}$$

Here, ω is the angular frequency, α is the exponent of the power law ($0 < \alpha < 1$), η is the structural damping coefficient defined as $\eta = \tan\frac{\pi\alpha}{2}$, $\Gamma(.)$ denotes the gamma function, and μ is the Newtonian viscous term. G_0 and ω_0 are two scaling factors for the storage modulus and the angular frequency, respectively. Later, it was shown that such a power law based rheological behavior can also be described using fractional derivatives [164]. For example, a fractional Kelvin-Voigt rheological model can be described as:

$$\tilde{\boldsymbol{\sigma}}_{\boldsymbol{KVM}}(t) = G_s\tilde{\boldsymbol{\varepsilon}}_{\boldsymbol{KVM}}(t) + \eta_\alpha D^\alpha(\tilde{\boldsymbol{\varepsilon}}_{\boldsymbol{KVM}}(t)), \tag{10.11}$$

where $\tilde{\boldsymbol{\sigma}}_{\boldsymbol{KVM}}(t)$ denotes stress, G_s is the elastic shear modulus, $\tilde{\boldsymbol{\varepsilon}}_{\boldsymbol{KVM}}(t)$ corresponds to strain, and η_α describes the effective modulus. The fractional derivate is given by $D^\alpha\tilde{\varepsilon}(t) = \frac{d^\alpha\tilde{\varepsilon}(t)}{dt^\alpha}$, where its order α is the damping coefficient of the system structural changes. For simulating oscillatory behavior of airway smooth muscle cells, following expressions can be derived from the above equation [164]:

$$G'(\omega) = G_s + \eta_\alpha\omega^\alpha\cos\left(\frac{\pi\alpha}{2}\right), \text{ and} \tag{10.12}$$

$$G''(\omega) = \eta_\alpha \omega^\alpha \sin\left(\frac{\pi\alpha}{2}\right). \tag{10.13}$$

Furthermore, adherent cells exhibit a proportionality behavior with the contractile stress, that is, their dynamic moduli increase with an increase in the contractile stress. The power law structural model is also utilized to quantify cell to cell variation in power law rheology [165] or to study temporal evolution of a single-cell rheology [166].

10.4.2.4 Biphasic model

Solid models discussed in previous sections consider cells to be in a single-phase material. However, many cells are often in two phases even in a steady state. For example, the cytoplasm consists both in solid polymeric contents and an interstitial fluid. Thus the two phases must be treated separately in such conditions. Thus a biphasic model [167] was introduced to consider the viscoelasticity in cells that are made of constituents in two phases, and for which, the liquid phase may diffuse through the solid phase. This theory was applied to study musculoskeletal cell mechanics and to model a single-chondrocyte subject to a flat punch indentation. In such a model, the solid phase is considered to be linearly elastic and the fluid phase is assumed to be an in viscid fluid.

The biphasic theory implies that cells and tissues exhibit viscoelastic behavior due to momentum exchange between the liquid and solid phases. Due to this complex behavior and the irregular geometry, developing a perfect analytical solution for a biphasic theory is very demanding. Nonetheless, the stress in the solid and liquid phases for the biphasic model can be computed as:

$$\sigma^s = -\phi^s p\mathbf{I} + \lambda_s tr(\varepsilon)\mathbf{I} + 2\mu_s \varepsilon, \tag{10.14}$$

$$\sigma^f = -\phi^f p\mathbf{I}. \tag{10.15}$$

Herein, σ^s and σ^f are the Causchy stress tensor for the solid and liquid phases, respectively, ϕ^s and ϕ^f are the solid and fluid volumetric functions ($\phi^s + \phi^f = 1$), p is the fluid pressure, $\mathbf{I}$ is the identity tensor, λ_s and μ_s are Lamé constants for the solid phase, and $tr(\varepsilon)$ is the trace of the Cauchy's infinitesimal strain tensor. A study based on a microindentation approach showed that a nonlinear biphasic model best represents the time-dependent mechanical behavior of articular cartilages [168]. The biphasic properties of single-bone cells and cartilages were utilized to characterize the dynamic environment of the surrounding ECM around chondrocytes in studying mechanotransduction of chondrocytes and the mechanobiology of the cartilage [169,170]. However, the fluid barrier behavior of the plasma membrane is not explored in detail, which is an important step in further developing more realistic cell models.

10.5 Trends in viscoelastography

Thus far, the viscoelastic nature of cells has been alluded to. Despite early working confirming this nature, microrheology measurements of viscoelasticity are scarce with most methods only capturing the elasticity. This is because at long time-scales (≥ 1 ms), the elastic response dominates [163,171,172]. It is thus necessary to develop techniques with higher temporal resolution (higher probing frequencies) to achieve a more comprehensive mechanical phenotype of the intact cell. Additionally, this would be advantageous for elucidating dynamic processes that occur in a small time scale. Demonstratively, Rigato et al. [171] successfully conducted high frequency ($1-100$ kHz) microrheology experiments using AFM. High-speed AFM is adapted with a miniature piezoelectric element with a resonant frequency of 200 kHz, and cells are visualized by transmission microscopy. Active rheology performed across the frequency range revealed that storage and loss moduli of fibroblasts increased in a similar way up to about 300 Hz after which, the loss modulus had a faster rate and finally became greater than the storage modulus above 30 kHz. Following, low and high viscoelastic regimes were identified, characterizing a purely viscous behavior or a fluid response with a transition frequency of 84 kHz for fibroblasts [171]. These results give access to the characterization of mechanical phenotypes of cells, both static and dynamic states, as well as the morphology. The authors demonstrated the utility of high-frequency imaging by charactering cells with a manipulated CSK architecture, confirming the role of the CSK in cellular biomechanics showing that cells with different CSK arrangements have unique mechanical properties. Moreover, they demonstrated the utility of high-frequency imaging in distinguishing the phenotype of benign and malignant breast cancer cells, posing viscoelasticity as a powerful biomarker.

The promise of frequency-based rheology is further demonstrated by Grasland-Mongrain et al. [112], who developed an ultrafast imaging system with optical microscopy. By inducing a high-frequency (15 kHz) shear wave within mammalian oocytes, the wave propagation could be followed using an ultrafast camera (200,000 frames per second). From the image cineloop, the elastic modulus of the whole cell was extracted by tracking the displacement of the wave, frame to frame, allowing the generation of elastic maps. The high spatial resolution gave access to zonal classification allowing mapping elasticity of the extracellular fluid, zona pellicuda, cytoplasm, and nucleus, providing more support for the mechanical heterogeneity of cells. Imaging whole cells without any chemical manipulation greatly opens the potential for longitudinal imaging, demonstrated by the same authors who imaged the oocyte at different maturation stages. Although results are in two dimensions, the method is extendable to three dimensions by focusing the camera at different depths. Additionally, the method may extract viscous properties by incorporating shear wave attenuation tracking capabilities [173]. Verified by simulation results, this method is reasonably accurate with high spatial and temporal resolutions.

To optimize such high-frequency rheological techniques, reducing the number of approximations would be beneficial. Model-independent rheology has been suggested to quantify the viscoelasticity of biological tissues by Kazemirad et al. [111] based on the propagation of shear waves. Following Navier's equation that governs the wave motion, a solution to the inverse wave propagation problem was analytically developed; from which both storage (elastic) and loss (viscous) moduli were obtained for in vitro and ex vivo porcine liver samples over a broad frequency range. Eliminating the need for a model describing the tissue (or cell) reduces inaccuracies due to rheology approximations and assumptions, thus a more direct mechanical phenotype might be obtained. Despite this success, the method [111] carries its own limiting assumptions that is by basing the analytical solution on Navier's equation, they inherently assume the wave to propagate in isotropic, linear, and homogeneous media. This method is best suited for macroscopic homogenous samples. Within the cell, homogeneity does not hold based on structural and content differences, for example, the isolated nucleus being stiffer and more viscous than the intact cell [142], and cortex mechanics dominating over cytoplasm during mitosis [174]. Nonetheless, the development of model-independent rheology techniques that consider heterogeneous samples is a promising path in elucidating the viscoelastic nature of cells, while minimizing approximations necessary.

Most imaging techniques focus on single cells, however, these methods may be limited in clinical applications where a single sample may contain thousands or millions of cells. For example, a biopsy sample may contain thousands of normal cells and only a small percentage of malignant cells. Processing such a sample one cell at a time is inefficient given that physical properties of cells could be altered in the external environment of buffer or media. High-throughput methods are thus necessary to efficiently translate viscoelasticity as a biomarker to clinical applications. The emerging tools are variant in throughput rates ranging from 1 cell/minute to 20,000 cells/second [175]. Adapting single-cell methods to high-throughput applications would be the natural first step. Optical trapping is one such technique whose utility has been stretched to characterize a large number of cells. Measuring cells in rapid succession, by flushing them through a microfluidic channel through an optical trap, allowed statistically relevant numbers of single-cell analyses, yielding rates of approximately 1 cell/second to 20 cells/second [176,177]. Increasing the throughput rate of the experimentally ubiquitous AFM is limited largely by the time taken for the indentation process. However, a promising approach made use of a feedback system where the information from microscopic images would allow robotic positioning [178]. Automation of the scan through registration of cells relatively increased the speed to 3 seconds/cell; however this method is still riddled by the indentation time, thus it has not been pursued largely. Perhaps, opportunity for machine-learning approaches to increase efficiency of registration may occur.

Impressive throughput rates have been achieved by hydrodynamic and transit through constriction methods. Hydrodynamic approaches rely on intrinsic fluid-dynamic stresses that are regulated by the design of the microfluidic channels, yielding rates of up to 20,000 cells/second [179]. These channels can be divided into two designs, those that support lift of cells induced by the deformability in flow [180,181] and imaging of hydrodynamic-stretched cells [179,182–184]. A major limitation is that these methods highly depend on the cell shape and size, thus altered shapes and sizes cannot be captured within the same measurement. Transit through constriction methods are explained in the naming, where changes in cell size and shape are measured as cells travel through pores [175]. Achievements of this method include rates of 1 cell/second to 100 cells/

second depending on the automation. Automation can occur on readout methods, that is, by implementing high-speed imaging or higher precision sensing cantilever [185–190]. Improved automation may consequent in improved throughput rates. Given that the constriction size has to be calibrated to the size of the cell of interest, this technique is limited to homogenously sized cells. Beyond calibration to the cell of interest, most of high-throughput techniques are promising in efficiently translating viscoelastic measurements to clinical adaptations where processing millions of cells from a sample is necessary. Success in using the label-free mechanical biomarker would lead to more accurate phenotypes based on the natural state of the cell.

10.6 Summary

The living cell is a mechanical structure with the ability to detect external forces, internal forces from reorganization of subcellular structures and generate responsive forces that maintain functionality or induce growth and motility. The ability to survive mechanical changes largely depends on the deformability of cells, that is, elasticity, where increased or decreased elasticity can inform on the pathophysiological state. In fact, numerous disease states and developmental abnormalities clinically manifest as reduced elasticity or heightened stiffness in whole organs or tissues. Tissues and organs are fundamentally constituted of a collection of cells, thus by assessing the elasticity of single cells, a label-free biomarker informative of the disease state, functionality, and developmental status can be developed.

Methods to quantify the elasticity of cells are developed and emerging trends attempt to increase spatial and temporal resolutions. Increased spatial resolution makes accessible subcellular structures with techniques increasingly being able to distinguish the mechanical contribution of distinct structures such as the membrane, CSK, and the nucleus, whereas increased temporal resolution captures dynamic changes that rapidly occur. Most rheological techniques rely on a model to verify experimental results through simulations. Choosing a technique and accompanying model largely depends on approximations within reach and their appropriateness to the cell being studied. Variations in cell shape, size, nucleation, adhesive properties, and function dictate the choices in measuring techniques.

Elasticity alone as a biomechanical marker can result in ambiguous characterization, as cells are not entirely solid structures. The presence of a cytoplasm filled with the fluid-like cytosol gives it viscous property. Viscoelasticity is thus necessary to accurately represent the mechanical phenotype of the cell. Of late, frequency-based techniques are most promising in quantifying viscoelasticity with the development of higher frequency methods within which the viscous nature is measurable. Moreover, to reduce the number of approximations, model-independent techniques have been developed of late, aiming to reduce inaccuracies introduced by fitting experimental results to a model. The overall goal of cellular imaging is in determining functional, pathophysiological, and developmental states of living cells. If such techniques are to be translated to clinical applications, increased efficiency in the number of cells processed is necessary as biological samples typically include thousands or millions of cells. High-throughput techniques are a recent topic of interest, whether it includes adapting single cellular techniques or developing new rheological approaches. Recently, the viscoelasticity of cells could be quantified at the impressive rate of 20,000 cells/second through hydrodynamic approaches.

Acknowledgment

We would like to thank Rodin Chemalat, Thomas Gibaud, and Thomas Dehoux for useful discussions about cell structure, microrheology, and Brillouin scattering, respectively. Partial funding for the cell microelastography work was obtained from a Strategic grant of the Quebec Bioimaging Network.

References

[1] S.-Y. Tee, A.R. Bausch, P.A. Janmey, The mechanical cell, Curr. Biol. 19 (17) (2009) R745–R748.

[2] M. Khalilian, et al., Alteration in the mechanical properties of human ovum zona pellucida following fertilization: experimental and analytical studies, Exp. Mech. 51 (2) (2011) 175–182.

[3] G.Y. Lee, C.T. Lim, Biomechanics approaches to studying human diseases, Trends Biotechnol. 25 (3) (2007) 111–118.

[4] P. Carl, H. Schillers, Elasticity measurement of living cells with an atomic force microscope: data acquisition and processing, Pflug. Arch. 457 (2) (2008) 551–559.

[5] M.B. Ginzberg, R. Kafri, M. Kirschner, On being the right (cell) size, Science 348 (6236) (2015) 1245075.

[6] R. Changede, M. Sheetz, Integrin and cadherin clusters: a robust way to organize adhesions for cell mechanics, BioEssays 39 (1) (2017) 1–12.

[7] G. Karp, Cell and Molecular Biology: Concepts and Experiments, John Wiley & Sons, 2009.
[8] W. Helfrich, Elastic properties of lipid bilayers: theory and possible experiments, Z. für Naturforschung C. 28 (11-12) (1973) 693–703.
[9] W. Helfrich, Steric interaction of fluid membranes in multilayer systems, Z. für Naturforschung A 33 (3) (1978) 305–315.
[10] E.A. Evans, Bending resistance and chemically induced moments in membrane bilayers, Biophysical J. 14 (12) (1974) 923–931.
[11] C.C. DuFort, M.J. Paszek, V.M. Weaver, Balancing forces: architectural control of mechanotransduction, Nat. Rev. Mol. Cell Biol. 12 (5) (2011) 308–319.
[12] S. Kumar, et al., Viscoelastic retraction of single living stress fibers and its impact on cell shape, cytoskeletal organization, and extracellular matrix mechanics, Biophysical J. 90 (10) (2006) 3762–3773.
[13] T.P. Lele, et al., Mechanical forces alter zyxin unbinding kinetics within focal adhesions of living cells, J. Cell. Physiol. 207 (1) (2006) 187–194.
[14] C.-M. Lo, et al., Cell movement is guided by the rigidity of the substrate, Biophysical J. 79 (1) (2000) 144–152.
[15] B. Alberts, et al., Molecular Biology of the Cell: Reference Edition, Garland Science, 2007, p. 2.
[16] K. Sengupta, A.-S. Smith, Adhesion of biological membranes, in: P. Bassereau, P. Sens (Eds.), Physics of Biological Membranes, Springer International Publishing, Cham, 2018, pp. 499–535.
[17] J.Z. Kechagia, J. Ivaska, P. Roca-Cusachs, Integrins as biomechanical sensors of the microenvironment, Nat. Rev. Mol. Cell Biol. 20 (2019) 457–473.
[18] R.O. Hynes, Integrins: bidirectional, allosteric signaling machines, Cell 110 (6) (2002) 673–687.
[19] M. Kim, C.V. Carman, T.A. Springer, Bidirectional transmembrane signaling by cytoplasmic domain separation in integrins, Science 301 (5640) (2003) 1720–1725.
[20] J.D. Humphries, et al., Signal transduction via integrin adhesion complexes, Curr. Opin. Cell Biol. 56 (2019) 14–21.
[21] Z. Sun, S.S. Guo, R. Fässler, Integrin-mediated mechanotransduction, J. Cell Biol. 215 (4) (2016) 445–456.
[22] E. Sackmann, Advanced concepts and perspectives of membrane physics, in: P. Bassereau, P. Sens (Eds.), Physics of Biological Membranes, Springer International Publishing, Cham, 2018, pp. 45–70.
[23] A. Kusumi, et al., Dynamic organizing principles of the plasma membrane that regulate signal transduction: commemorating the fortieth anniversary of Singer and Nicolson's fluid-mosaic model, Annu. Rev. Cell Dev. Biol. 28 (2012) 215–250.
[24] M. Fritzsche, et al., Actin kinetics shapes cortical network structure and mechanics, Sci. Adv. 2 (4) (2016) e1501337.
[25] P. Sens, J. Plastino, Membrane tension and cytoskeleton organization in cell motility, J. Phys.: Condens. Matter 27 (27) (2015) 273103.
[26] H.M. Nussenzveig, Cell membrane biophysics with optical tweezers, Eur. Biophys. J. 47 (5) (2018) 499–514.
[27] K. Rottner, M. Schaks, Assembling actin filaments for protrusion, Curr. Opin. Cell Biol. 56 (2019) 53–63.
[28] A. Gefen, D. Weihs, Cytoskeleton and plasma-membrane damage resulting from exposure to sustained deformations: a review of the mechanobiology of chronic wounds, Med. Eng. Phys. 38 (9) (2016) 828–833.
[29] S. Boulant, et al., Actin dynamics counteract membrane tension during clathrin-mediated endocytosis, Nat. Cell Biol. 13 (9) (2011) 1124–1131.

[30] P.A. Janmey, C.A. McCulloch, Cell mechanics: integrating cell responses to mechanical stimuli, Annu. Rev. Biomed. Eng. 9 (1) (2007) 1−34.

[31] M. Enrique, M.L. Gardel, Actin mechanics and fragmentation, J. Biol. Chem. 290 (28) (2015) 17137−17144.

[32] G. Salbreux, G. Charras, E. Paluch, Actin cortex mechanics and cellular morphogenesis, Trends Cell Biol. 22 (10) (2012) 536−545.

[33] P. Kollmannsberger, B. Fabry, Linear and nonlinear rheology of living cells, Annu. Rev. Mater. Res. 41 (2011) 75−97.

[34] P. Isermann, J. Lammerding, Nuclear mechanics and mechanotransduction in health and disease, Curr. Biol. 23 (24) (2013) R1113−R1121.

[35] D. Ingber, Mechanobiology and diseases of mechanotransduction, Ann. Med. 35 (8) (2003) 564−577.

[36] M.M. Yallapu, et al., The roles of cellular nanomechanics in cancer, Med. Res. Rev. 35 (1) (2015) 198−223.

[37] C. Rianna, M. Radmacher, Cell mechanics as a marker for diseases: biomedical applications of AFM, AIP Conference Proceedings, AIP Publishing, 2016.

[38] G. Burgstaller, et al., The instructive extracellular matrix of the lung: basic composition and alterations in chronic lung disease, Eur. Respir. J. 50 (1) (2017) 1601805.

[39] J.K. Burgess, et al., The extracellular matrix—the under-recognized element in lung disease? J. Pathol. 240 (4) (2016) 397−409.

[40] J. Mead, I. Lindgren, E. Gaensler, The mechanical properties of the lungs in emphysema, J. Clin. Invest. 34 (7) (1955) 1005−1016.

[41] M. Lekka, et al., Elasticity of normal and cancerous human bladder cells studied by scanning force microscopy, Eur. Biophys. J. 28 (4) (1999) 312−316.

[42] J. Guck, et al., Optical deformability as an inherent cell marker for testing malignant transformation and metastatic competence, Biophys. J. 88 (5) (2005) 3689−3698.

[43] J.J. Fredberg, Frozen objects: small airways, big breaths, and asthma, J. Allergy Clin. Immunol. 106 (4) (2000) 615−624.

[44] J. Li, et al., Cytoskeletal dynamics of human erythrocyte, Proc. Natl Acad. Sci. U. S. A. 104 (12) (2007) 4937−4942.

[45] M. Puig-de-Morales-Marinkovic, et al., Viscoelasticity of the human red blood cell, Am. J. Physiol.-Cell Physiol. 293 (2) (2007) C597−C605.

[46] L. Wang, et al., Tissue and cellular rigidity and mechanosensitive signaling activation in Alexander disease, Nat. Commun. 9 (1) (2018) 1899.

[47] A.J. Booth, et al., Acellular normal and fibrotic human lung matrices as a culture system for in vitro investigation, Am. J. Respir. Crit. Care Med. 186 (9) (2012) 866−876.

[48] H. Parameswaran, A. Majumdar, B. Suki, Linking microscopic spatial patterns of tissue destruction in emphysema to macroscopic decline in stiffness using a 3D computational model, PLoS Comput. Biol. 7 (4) (2011) e1001125.

[49] R. Annoni, et al., Extracellular matrix composition in COPD, Eur. Respir. J. 40 (6) (2012) 1362−1373.

[50] Y.S. Oh, et al., A special report on the NHLBI initiative to study cellular and molecular mechanisms of arterial stiffness and its association with hypertension, Circ. Res. 121 (11) (2017) 1216−1218.

[51] S. Suresh, et al., Connections between single-cell biomechanics and human disease states: gastrointestinal cancer and malaria, Acta Biomater. 1 (1) (2005) 15−30.

[52] N. Schierbaum, J. Rheinlaender, T.E. Schäffer, Viscoelastic properties of normal and cancerous human breast cells are affected differently by contact to adjacent cells, Acta Biomater. 55 (2017) 239−248.

[53] L. Winter, W.H. Goldmann, Biomechanical characterization of myofibrillar myopathies, Cell Biol. Int. 39 (4) (2015) 361−363.

[54] R. Krishnan, et al., Cellular biomechanics in drug screening and evaluation: mechanopharmacology, Trends Pharmacol. Sci. 37 (2) (2016) 87−100.
[55] M. Li, et al., Nanoscale monitoring of drug actions on cell membrane using atomic force microscopy, Acta Pharmacol. Sin. 36 (7) (2015) 769−782.
[56] A.M. Kolodziejczyk, M. Targosz-Korecka, M. Szymonski, Nanomechanical testing of drug activities at the cellular level: case study for endothelium-targeted drugs, Pharmacol. Rep. 69 (6) (2017) 1165−1172.
[57] J.D. Mih, et al., A multiwell platform for studying stiffness-dependent cell biology, PLoS One 6 (5) (2011) e19929.
[58] S. Seyedpour, et al., Effects of an antimitotic drug on mechanical behaviours of the cytoskeleton in distinct grades of colon cancer cells, J. Biomech. 48 (6) (2015) 1172−1178.
[59] O.Y. Selyutina, et al., Influence of glycyrrhizin on permeability and elasticity of cell membrane: perspectives for drugs delivery, Drug Delivery 23 (3) (2016) 848−855.
[60] T. Auth, S. Dasgupta, G. Gompper, Interaction of particles and pathogens with biological membranes, Physics of Biological Membranes, Springer, 2018, pp. 471−498.
[61] M.J. Whitfield, J.P. Luo, W.E. Thomas, Yielding elastic tethers stabilize robust cell adhesion, PLoS Comput. Biol. 10 (12) (2014) e1003971.
[62] A. Persat, et al., The mechanical world of bacteria, Cell 161 (5) (2015) 988−997.
[63] M. Otto, Physical stress and bacterial colonization, FEMS Microbiol. Rev. 38 (6) (2014) 1250−1270.
[64] I. Tardieux, J. Baum, Reassessing the mechanics of parasite motility and host-cell invasion, J. Cell Biol. 214 (5) (2016) 507−515.
[65] A. Elbourne, et al., Bacterial-nanostructure interactions: the role of cell elasticity and adhesion forces, J. Colloid Interface Sci. 546 (2019) 192−210.
[66] R. Ebady, et al., Biomechanics of *Borrelia burgdorferi* vascular interactions, Cell Rep. 16 (10) (2016) 2593−2604.
[67] M.A. Dragovich, et al., Biomechanical characterization of TIM protein−mediated *Ebola* virus−host cell adhesion, Sci. Rep. 9 (1) (2019) 267.
[68] Y. Sun, T.-L. Sun, H.W. Huang, Physical properties of *Escherichia coli* spheroplast membranes, Biophys. J. 107 (9) (2014) 2082−2090.
[69] S. Hillringhaus, et al., Importance of erythrocyte deformability for the alignment of malaria parasite upon invasion, Biophys. J. 117 (2019) 1202−1214.
[70] S. Hasim, et al., β-(1, 3)-Glucan unmasking in some Candida albicans mutants correlates with increases in cell wall surface roughness and decreases in cell wall elasticity, Infect. Immun. 85 (1) (2017) e00601-16.
[71] M. Beckmann, et al., Measuring cell surface elasticity on enteroaggregative Escherichia coli wild type and dispersin mutant by AFM, Ultramicroscopy 106 (8-9) (2006) 695−702.
[72] N.M. Ayad, S. Kaushik, V.M. Weaver, Tissue mechanics, an important regulator of development and disease, Philos. Trans. R. Soc. B 374 (1779) (2019) 20180215.
[73] A. Elosegui-Artola, X. Trepat, P. Roca-Cusachs, Control of mechanotransduction by molecular clutch dynamics, Trends Cell Biol. 28 (5) (2018) 356−367.
[74] L. Chin, et al., Mechanotransduction in cancer, Curr. Opin. Chem. Eng. 11 (2016) 77−84.
[75] A.Y. Malkin, A.I. Isayev, Rheology: Concepts, Methods, and Applications, Elsevier, 2017.
[76] E. Evans, A.J.Bj Yeung, Apparent viscosity and cortical tension of blood granulocytes determined by micropipet aspiration, Biophys. J. 56 (1) (1989) 151−160.
[77] J.P. Brody, Y. Han, R.H. Austin, M. Bitensky, Deformation and flow of red blood cells in a synthetic lattice: evidence for an active cytoskeleton, Biophys. J. 68 (6) (1995) 2224−2232.

[78] W.A. Lam, M.J. Rosenbluth, D.A. Fletcher, Chemotherapy exposure increases leukemia cell stiffness, Blood 109 (8) (2007) 3505–3508.
[79] N. Wang, J.P. Butler, D.E. Ingber, Mechanotransduction across the cell surface and through the cytoskeleton, Science 260 (5111) (1993) 1124–1127.
[80] J. Guck, R. Ananthakrishnan, H. Mahmood, T.J. Moon, C.C. Cunningham, J. Käs, The optical stretcher: a novel laser tool to micromanipulate cells, Biophys. J. 81 (2) (2001) 767–784.
[81] M. Khalilian, M. Navidbakhsh, M.R. Valojerdi, M. Chizari, P.E. Yazdi, Estimating Young's modulus of zona pellucida by micropipette aspiration in combination with theoretical models of ovum, J. R. Soc. Interface 7 (45) (2009) 687–694.
[82] Y. Sun, K.T. Wan, K.P. Roberts, J.C. Bischof, B.J. Nelson, Mechanical property characterization of mouse zona pellucida, IEEE Trans. Nanobioscience 2 (4) (2003) 279–286.
[83] Y. Murayama, et al., Elasticity measurement of zona pellucida using a micro tactile sensor to evaluate embryo quality, J. Mammalian Ova Res. 25 (1) (2008) 8–16.
[84] A. Ashkin, J.M. Dziedzic, Optical trapping and manipulation of viruses and bacteria, Science 235 (4795) (1987) 1517–1520.
[85] A. Ashkin, K. Schütze, J.M. Dziedzic, U. Euteneuer, M. Schliwa, Force generation of organelle transport measured in vivo by an infrared laser trap, Nature 348 (6299) (1990) 346–348.
[86] S.M. Block, D.F. Blair, H.C. Berg, Compliance of bacterial flagella measured with optical tweezers, Nature 338 (6215) (1989) 514–518.
[87] J. Wu, Acoustical tweezers, J. Acoustical Soc. Am. 89 (5) (1991) 2140–2143.
[88] A. Ozcelik, J. Rufo, F. Guo, Y. Gu, P. Li, J. Lata, et al., Acoustic tweezers for the life sciences, Nat. Methods 15 (12) (2018) 1021–1028.
[89] A.R. Bausch, W. Möller, E. Sackmann, Measurement of local viscoelasticity and forces in living cells by magnetic tweezers, Biophys. J. 76 (1) (1999) 573–579.
[90] F.J. Alenghat, B. Fabry, K.Y. Tsai, W.H. Goldmann, D.E. Ingber, Analysis of cell mechanics in single vinculin-deficient cells using a magnetic tweezer, Biochem. Biophys. Res. Commun. 277 (1) (2000) 93–99.
[91] A. Emad, W.F. Heinz, M.D. Antonik, N.P. D'Costa, S. Nageswaran, C.A. Schoenenberger, et al., Relative microelastic mapping of living cells by atomic force microscopy, Biophys. J. 74 (3) (1998) 1564–1578.
[92] C.A. Putman, K.O. Van der Werf, B.G. de Grooth, N.F. van Hulst, J. Greve, Viscoelasticity of living cells allows high resolution imaging by tapping mode atomic force microscopy, Biophys. J. 67 (4) (1994) 1749–1753.
[93] M. Radmacher, R.W. Tillamnn, M. Fritz, H.E. Gaub, From molecules to cells: imaging soft samples with the atomic force microscope, Science 257 (5078) (1992) 1900–1905.
[94] X. Liu, J. Shi, Z. Zong, K.T. Wan, Y. Sun, Elastic and viscoelastic characterization of mouse oocytes using micropipette indentation, Ann. Biomed. Eng. 40 (10) (2010) 2122–2130.
[95] M. Radmacher, M. Fritz, C.M. Kacher, J.P. Cleveland, P.K. Hansma, Measuring the viscoelastic properties of human platelets with the atomic force microscope, Biophys. J. 70 (1) (1996) 556–567.
[96] T.G. Mason, K. Ganesan, J.H. Van Zanten, D. Wirtz, S.C. Kuo, Particle tracking microrheology of complex fluids, Phys. Rev. Lett. 79 (17) (1997) 3282–3285.
[97] J.C. Crocker, M.T. Valentine, E.R. Weeks, T. Gisler, P.D. Kaplan, A.G. Yodh, et al., Two-point microrheology of inhomogeneous soft materials, Phys. Rev. Lett. 85 (4) (2000) 888–891.
[98] B. Fabry, et al., Time scale and other invariants of integrative mechanical behavior in living cells, Phys. Rev. E 68 (4) (2003) 041914.

[99] G.N. Maksym, B. Fabry, J.P. Butler, D. Navajas, D.J. Tschumperlin, J.D. Laporte, et al., Mechanical properties of cultured human airway smooth muscle cells from 0.05 to 0.4 Hz, J. Appl. Physiol. 89 (4) (2000) 1619−1632.
[100] Y. Tseng, T.P. Kole, D. Wirtz, Micromechanical mapping of live cells by multiple-particle-tracking microrheology, Biophys. J. 83 (6) (2002) 3162−3176.
[101] Y. Tseng, J.S. Lee, T.P. Kole, I. Jiang, D. Wirtz, Micro-organization and visco-elasticity of the interphase nucleus revealed by particle nanotracking, J. Cell Sci. 117 (10) (2004) 2159−2167.
[102] G. Scarcelli, W.J. Polacheck, H.T. Nia, K. Patel, A.J. Grodzinsky, R.D. Kamm, et al., Noncontact three-dimensional mapping of intracellular hydromechanical properties by Brillouin microscopy, Nat. Methods 12 (12) (2015) 1132−1134.
[103] G. Scarcelli, S.H. Yun, Confocal Brillouin microscopy for three-dimensional mechanical imaging, Nat. Photonics 2 (1) (2008) 39−43.
[104] P.J. Wu, et al., Water content, not stiffness, dominates Brillouin spectroscopy measurements in hydrated materials, Nat. Methods 15 (8) (2018) 561−562.
[105] T.A. Krouskop, D.R. Dougherty, F.S. Vinson, A pulsed Doppler ultrasonic system for making noninvasive measurements of the mechanical properties of soft tissue, J. Rehabilitation Res. Dev. 24 (2) (1987) 1−8.
[106] S. Catheline, F. Yu, M. Fink, A solution to diffraction biases in sonoelasticity: the acoustic impulse technique, J. Acoustical Soc. Am. 105 (5) (1999) 2941−2950.
[107] R. Muthupillai, P.J. Rossman, D.J. Lomas, J.F. Greenleaf, S.J. Riederer, R.L. Ehman, Magnetic resonance imaging of transverse acoustic strain waves, Magnetic Reson. Med. 36 (2) (1996) 266−274.
[108] L. Sandrin, et al., Transient elastography: a new noninvasive method for assessment of hepatic fibrosis, Ultrasound Med. Biol. 29 (12) (2003) 1705−1713.
[109] J. Bercoff, et al., In vivo breast tumor detection using transient elastography, Ultrasound Med. Biol. 29 (10) (2003) 1387−1396.
[110] F. Sebag, J. Vaillant-Lombard, J. Berbis, V. Griset, J.F. Henry, P. Petit, et al., Shear wave elastography: a new ultrasound imaging mode for the differential diagnosis of benign and malignant thyroid nodules, J. Clin. Endocrinol. Metab. 95 (12) (2010) 5281−5288.
[111] S. Kazemirad, S. Bernard, S. Hybois, A. Tang, G. Cloutier, Ultrasound shear wave viscoelastography: model-independent quantification of the complex shear modulus, IEEE Trans. Ultrasonics, Ferroelectrics, Frequency Control. 63 (9) (2016) 1399−1408.
[112] P. Grasland-Mongrain, A. Zorgani, S. Nakagawa, S. Bernard, L. Gomes Paim, G. Fitzharris, S. Catheline, G. Cloutier, Ultrafast imaging of cell elasticity with optical microelastography, Proc. Natl Acad. Sci. U. S. A. 115 (5) (2018) 861−866.
[113] M.M. Brandao, A. Fontes, M.L. Barjas-Castro, L.C. Barbosa, F.F. Costa, C.L. Cesar, et al., Optical tweezers for measuring red blood cell elasticity: application to the study of drug response in sickle cell disease, Eur. J. Haematol. 70 (4) (2003) 207−211.
[114] L. Tetard, A. Passian, R.M. Lynch, B.H. Voy, G. Shekhawat, V. Dravid, et al., Elastic phase response of silica nanoparticles buried in soft matter, Appl. Phys. Lett. 93 (13) (2008) 133113.
[115] C.T. Lim, E.H. Zhou, S.T. Quek, Mechanical models for living cells—a review, J. Biomech. 39 (2) (2006) 195−216.
[116] J. Chen, Nanobiomechanics of living cells: a review, Interface Focus. 4 (2) (2014) 20130055.
[117] B. Fuller, Tensegrity. Portfolio and Art News Annual. 1961.
[118] F.R. Buckminster, Tensile-integrity structures. 1962, Google Patents.

[119] R.E. Skelton, et al., An introduction to the mechanics of tensegrity structures. in Proceedings of the 40th IEEE Conference on Decision and Control (Cat. No. 01CH37228). 2001. IEEE.

[120] D.E. Ingber, Tensegrity: the architectural basis of cellular mechanotransduction, Annu. Rev. Physiol. 59 (1) (1997) 575–599.

[121] D.E. Ingber, Cellular tensegrity: defining new rules of biological design that govern the cytoskeleton, J. Cell Sci. 104 (3) (1993) 613–627.

[122] L. Wang, W. Chen, Modelling cell origami via a tensegrity model of the cytoskeleton in adherent cells, Appl. Bionics Biomech. (2019) 8541303.

[123] K.Y. Volokh, On tensegrity in cell mechanics, Mol. Cell. Biomech. 8 (2011) 195–214.

[124] D.E. Ingber, N. Wang, D. Stamenović, Tensegrity, cellular biophysics, and the mechanics of living systems, Rep. Prog. Phys. 77 (4) (2014) 046603.

[125] D. Stamenović, M.F. Coughlin, The role of prestress and architecture of the cytoskeleton and deformability of cytoskeletal filaments in mechanics of adherent cells: a quantitative analysis, J. Theor. Biol. 201 (1) (1999) 63–74.

[126] M.F. Coughlin, D. Stamenovic, A quantitative model of cellular elasticity based on tensegrity, J. Biomech. Eng. 122 (1) (2000) 39–43.

[127] P. Canadas, et al., A cellular tensegrity model to analyse the structural viscoelasticity of the cytoskeleton, J. Theor. Biol. 218 (2) (2002) 155–173.

[128] G.-K. Xu, et al., A tensegrity model of cell reorientation on cyclically stretched substrates, Biophys. J. 111 (7) (2016) 1478–1486.

[129] N. Bonakdar, et al., Mechanical plasticity of cells, Nat. Mater. 15 (10) (2016) 1090–1094.

[130] L. Zhang, X. Feng, S. Li, Review and perspective on soft matter modeling in cellular mechanobiology: cell contact, adhesion, mechanosensing, and motility, Acta Mech. 228 (12) (2017) 4095–4122.

[131] M. Fraldi, et al., Buckling soft tensegrities: Fickle elasticity and configurational switching in living cells, J. Mech. Phys. Solids 124 (2019) 299–324.

[132] Y.D. Bansod, et al., A finite element bendo-tensegrity model of eukaryotic cell, J. Biomech. Eng. 140 (10) (2018) 101001.

[133] G. Forgacs, On the possible role of cytoskeletal filamentous networks in intracellular signaling: an approach based on percolation, J. Cell Sci. 108 (6) (1995) 2131–2143.

[134] M.J. Saxton, The membrane skeleton of erythrocytes. A percolation model, Biophys. J. 57 (6) (1990) 1167–1177.

[135] D. Stamenović, D.E. Ingber, Models of cytoskeletal mechanics of adherent cells, Biomech. Modeling Mechanobiol. 1 (1) (2002) 95–108.

[136] T.G. Fai, et al., Image-based model of the spectrin cytoskeleton for red blood cell simulation, PLoS Comput. Biol. 13 (10) (2017) e1005790.

[137] V. Privman, et al., Lattice percolation approach to numerical modelling of tissue aging, Int. J. Parallel, Emergent Distrib. Syst. 31 (1) (2016) 1–19.

[138] E. Evans, B. Kukan, Passive material behavior of granulocytes based on large deformation and recovery after deformation tests, Blood 64 (5) (1984) 1028–1035.

[139] G. Schmid-Schonbein, Y.Y. Shih, S.J.B. Chien, Morphometry of human leukocytes, Blood 56 (5) (1980) 866–875.

[140] D. Needham, R.M. Hochmuth, A sensitive measure of surface stress in the resting neutrophil, Biophys. J. 61 (6) (1992) 1664–1670.

[141] C. Dong, R. Skalak, K.L. Sung, Cytoplasmic rheology of passive neutrophils, Biorheology 28 (6) (1991) 557–567.

[142] F. Guilak, et al., Viscoelastic properties of the cell nucleus, Biochem. Biophys. Res. Commun. 269 (3) (2000) 781–786.

[143] N. Caille, et al., Contribution of the nucleus to the mechanical properties of endothelial cells, J. Biomech. 35 (2) (2002) 177–187.

[144] H.-C. Kan, et al., Hydrodynamics of a compound drop with application to leukocyte modeling, Phys. Fluids 10 (4) (1998) 760–774.

[145] R. Tran-Son-Tay, et al., Time-dependent recovery of passive neutrophils after large deformation, Biophys. J. 60 (4) (1991) 856–866.

[146] R. Hochmuth, et al., Viscosity of passive human neutrophils undergoing small deformations, Biophys. J. 64 (5) (1993) 1596–1601.

[147] R. Tran-Son-Tay, et al., Rheological modelling of leukocytes, Med. Biol. Eng. Comput. 36 (2) (1998) 246–250.

[148] M.A. Tsai, R.S. Frank, R.E.J.Bj Waugh, Passive mechanical behavior of human neutrophils: power-law fluid, Biophys. J. 65 (5) (1993) 2078–2088.

[149] J.L. Drury, M.J.Bj Dembo, Hydrodynamics of micropipette aspiration, Biophys. J. 76 (1) (1999) 110–128.

[150] J.L. Drury, M. Dembo, Aspiration of human neutrophils: effects of shear thinning and cortical dissipation, Biophys. J. 81 (6) (2001) 3166–3177.

[151] C. Dong, et al., Passive deformation analysis of human leukocytes, J. Biomech. Eng. 110 (1) (1988) 27–36.

[152] C. Dong, R. Skalak, Leukocyte deformability: finite element modeling of large viscoelastic deformation, J. Theor. Biol. 158 (2) (1992) 173–193.

[153] J.D. Ferry, Viscoelastic Properties of Polymers, John Wiley & Sons, 1980.

[154] D.P. Theret, M.J. Levesque, M. Sato, R.M. Nerem, L.T. Wheeler, The application of a homogeneous half-space model in the analysis of endothelial cell micropipette measurements, J. Biochem. Eng. 110 (3) (1988) 190–199.

[155] W.R. Jones, et al., Alterations in the Young's modulus and volumetric properties of chondrocytes isolated from normal and osteoarthritic human cartilage, J. Biomech. 32 (2) (1999) 119–127.

[156] G.G. Bilodeau, Regular pyramid punch problem, J. Mech. Phys. Solids 59 (3) (1992) 519–523.

[157] S.M. Mijailovich, et al., A finite element model of cell deformation during magnetic bead twisting, J. Appl. Physiol. 93 (4) (2002) 1429–1436.

[158] M. Sato, D.P. Theret, L.T. Wheeler, N. Ohshima, R.M. Nerem, Application of the micropipette technique to the measurement of cultured porcine aortic endothelial cell viscoelastic properties, J. Biochem. Eng. 112 (3) (1990) 263–268.

[159] E.J. Koay, A.C. Shieh, K.A. Athanasiou, Creep indentation of single cells, J. Biomech. Eng. 125 (3) (2003) 334–341.

[160] M.A. Haider, F. Guilak, An axisymmetric boundary integral model for incompressible linear viscoelasticity: application to the micropipette aspiration contact problem, J. Biomech. Eng. 122 (3) (2000) 236–244.

[161] P.I. Milner, R.J. Wilkins, J.S. Gibson, Cellular physiology of articular cartilage in health and disease, Principles of Osteoarthritis-Its Definition, Character, Derivation and Modality-Related Recognition, IntechOpen, 2012.

[162] J. Alcaraz, et al., Microrheology of human lung epithelial cells measured by atomic force microscopy, Biophys. J. 84 (3) (2003) 2071–2079.

[163] B. Fabry, et al., Scaling the microrheology of living cells, Phys. Rev. Lett. 87 (14) (2001) 148102.

[164] V.D. Djordjevic, et al., Fractional derivatives embody essential features of cell rheological behavior, Ann. Biomed. Eng. 31 (6) (2003) 692–699.

[165] P. Cai, et al., Quantifying cell-to-cell variation in power-law rheology, Biophys. J. 105 (5) (2013) 1093–1102.

[166] P. Cai, et al., Temporal variation in single-cell power-law rheology spans the ensemble variation of cell population, Biophys. J. 113 (3) (2017) 671–678.

[167] V.C. Mow, S.C. Kuei, W.M. Lai, C.G. Armstrong, Biphasic creep and stress relaxation of articular cartilage in compression: theory and experiments, J. Biomech. Eng. 102 (1) (1980) 73−84.

[168] J.A. Wahlquist, et al., Indentation mapping revealed poroelastic, but not viscoelastic, properties spanning native zonal articular cartilage, Acta Biomater. 64 (2017) 41−49.

[169] J.Z. Wu, W. Herzog, M. Epstein, Modelling of location- and time-dependent deformation of chondrocytes during cartilage loading, J. Biomech. 32 (6) (1999) 563−572.

[170] F. Guilak, V.C. Mow, The mechanical environment of the chondrocyte: a biphasic finite element model of cell-matrix interactions in articular cartilage, J. Biomech. 33 (12) (2000) 1663−1673.

[171] A. Rigato, et al., High-frequency microrheology reveals cytoskeleton dynamics in living cells, Nat. Phys. 13 (8) (2017) 771−775.

[172] L. Deng, et al., Fast and slow dynamics of the cytoskeleton, Nat. Mater. 5 (8) (2006) 636−640.

[173] S. Bernard, S. Kazemirad, G. Cloutier, A frequency-shift method to measure shear-wave attenuation in soft tissues, IEEE Trans. Ultrasonics, Ferroelectrics, Frequency Control. 64 (3) (2017) 514−524.

[174] E. Fischer-Friedrich, et al., Rheology of the active cell cortex in mitosis, Biophys. J. 111 (3) (2016) 589−600.

[175] E.M. Darling, D. Di Carlo, High-throughput assessment of cellular mechanical properties, Annu. Rev. Biomed. Eng. 17 (2015) 35−62.

[176] I. Sraj, et al., Cell deformation cytometry using diode-bar optical stretchers, J. Biomed. Opt. 15 (4) (2010) 047010.

[177] T. Sawetzki, et al., Viscoelasticity as a biomarker for high-throughput flow cytometry, Biophys. J. 105 (10) (2013) 2281−2288.

[178] Z. Wang, et al., A fully automated system for measuring cellular mechanical properties, J. Laboratory Autom. 17 (6) (2012) 443−448.

[179] J.S. Dudani, et al., Pinched-flow hydrodynamic stretching of single-cells, Lab. a Chip 13 (18) (2013) 3728−3734.

[180] H. Amini, W. Lee, D. Di Carlo, Inertial microfluidic physics, Lab. a Chip 14 (15) (2014) 2739−2761.

[181] S.C. Hur, et al., Deformability-based cell classification and enrichment using inertial microfluidics, Lab. a Chip 11 (5) (2011) 912−920.

[182] D. Di Carlo, et al., Continuous inertial focusing, ordering, and separation of particles in microchannels, Proc. Natl Acad. Sci. U. S. A. 104 (48) (2007) 18892−18897.

[183] S. Cha, et al., Cell stretching measurement utilizing viscoelastic particle focusing, Anal. Chem. 84 (23) (2012) 10471−10477.

[184] Y. Zheng, et al., Characterization of red blood cell deformability change during blood storage, Lab. a Chip 14 (3) (2013) 577−583.

[185] A. Adamo, et al., Microfluidics-based assessment of cell deformability, Anal. Chem. 84 (15) (2012) 6438−6443.

[186] S. Byun, et al., Characterizing deformability and surface friction of cancer cells, Proc. Natl Acad. Sci. U. S. A. 110 (19) (2013) 7580−7585.

[187] J. Chen, et al., Classification of cell types using a microfluidic device for mechanical and electrical measurement on single cells, Lab. a Chip 11 (18) (2011) 3174−3181.

[188] H. Bow, et al., A microfabricated deformability-based flow cytometer with application to malaria, Lab. a Chip 11 (6) (2011) 1065−1073.

[189] A.C. Rowat, et al., Nuclear envelope composition determines the ability of neutrophil-type cells to passage through micron-scale constrictions, J. Biol. Chem. 288 (12) (2013) 8610−8618.

[190] O. Otto, et al., Real-time deformability cytometry: on-the-fly cell mechanical phenotyping, Nat. Methods 12 (3) (2015) 199−202.

Index

Note: Page numbers followed by "*f*" and "*t*" refer to figures and tables, respectively.

A

Acoustic scattering, 52
Actin-binding proteins (ABPs), 54–56
Actin cytoskeleton, 57–58, 64
  elastic and viscous components in actin networks, 54–56
  epithelia, actin architecture in, 58–59
  single-cell migration, actin architecture, 56–58
Actin networks, 58–59
  elastic and viscous components, 54–56
Active microrheology, 266–267
Actomyosin prestress, 64
Adherens junctions (AJs), 6, 9–10, 64, 89–90, 92
Aggregate pulsation/shivering, 210–212
α-actinin, 55
Animal pole, 137–139
Aspiration force and surface tension, 201–203
Atomic force microscopy (AFM), 50–51, 56–57, 264, 266, 267*f*, 280–281

B

Biochemical driving force, 243–245
Biointerface
  finite, 235–238
  sharp, 232–235
Biological viscoelasticity, measuring, 49–54
  experimental methods, 50–52
    noninvasive measurement tools, 52
    subcellular scale measurement tools, 50–51
    tissue-scale measurement tools, 51–52
    whole-cell measurement tools, 51
  viscoelastic properties extraction from experimental measurements, 52–54
Biophysical origins of viscoelasticity during CCM, 47
  cell–cell adhesion dynamics, 64–66
  cell–substrate adhesions and force transmission during migration, 59–61
  measuring biological viscoelasticity, 49–54
    experimental methods, 50–52
    viscoelastic properties extraction from experimental measurements, 52–54
  substrate mechanics during migration, 61–64
  timescale-dependent behavior in viscoelastic materials, 48
  viscoelasticity in collective tissue migration, 66–68
  viscoelasticity of the actin cytoskeleton, 54–59
    actin architecture during single-cell migration, 56–58
    actin architecture in epithelia, 58–59
Biphasic model, 282–283
Blastula, 137–139
Blebbistatin, 177–178
Borrelia burgdorferi, 263–264
Breathing oscillations, 170–172
Brillouin microscopy, 52
Brillouin scattering microscopy, 268, 269*f*

C

Cadherin-based adhesions, 64
Cadherin dynamics, 64–65
Caenorhabditis elegans, 57–58
Cancer cells, matching viscoelasticity in, 92–93
Candida albicans, 263–264
Catch bonds, 59
Cauchy's infinitesimal strain tensor, 282–283
CD44, 61

Cell aggregate micropipette aspiration, 41–42, 227, 228*f*
Cell aggregate uniaxial compression, 227, 228*f*
Cell biomechanics, 270
Cell–cell adherens junctions, 9–11
Cell–cell adhesion dynamics, 64–66
Cell–cell adhesions, 47
Cell–cell gap junctions, 8–9
Cell–cell junction dynamics, 64, 65*f*
Cell–cell junctions, 7, 8*f*, 164
  modifying, 89–90
  tight junctions (TJs), 11–12
Cell elasticity, 257
  estimation measured by, 264–271
    atomic force microscopy (AFM), 266, 267*f*
    Brillouin scattering microscopy, 268, 269*f*
    cellular deformation, 265
    cellular deformation using tweezers, 265–266
    microelastography, 268–270, 271*f*
    microrheology, 266–268, 268*f*
  single cell, rheological modeling of, 272–283
    continuum-based models, 275–283
    structure-based models, 272–275
  viscoelastography, trends in, 283–286
Cell–medium interface, 146
Cell migration, 47
Cell structure, 260–264
  cell membrane, 260–261
  clinical relevance of cellular elasticity, 262–264
  cytoplasm, 261–262
  nucleus, 262
Cell–substrate adhesions and force transmission during migration, 59–61
Cellular aggregates
  active response to mechanical stimuli, 210–215
    aggregate pulsation/shivering, 210–212, 211*f*
    delayed cell contraction, model of, 212–215
  permeability of, 215–218, 216*f*
  viscoelastic behavior of, 200–210, 202*f*
    aspiration force and surface tension, 201–203
    elastic deformation, 203–204
    murin sarcoma cell aggregates, rheological parameters for, 208–210
    rheological models for aggregate flow into the capillary, 206–208
    viscous dissipation, 204–205
Cellular components, viscoelasticity of, 80–84
Cellular level, effective inertia at, 180–181
Cellular mechanosensitivity, 210
Cellular viscoelastic behavior, 49–50
Challenging environments, collective cell migration in, 80
Characteristic equilibrium, 247, 248*t*
Clathrin, 61
Claudin-1, 11–12
Collagen-I, 63–64
Collective cell migration (CCM), defined, 1
Collective cell motion, mechanism of, 158–160
  collective cell migration, 159
  density, role of, 159–160
  mechanical machinery, 158–159
Collective migration, 58
Collective migratory cells, 90–91
Collective tissue migration, viscoelasticity in, 66–68
Connexons, 8–9
Constitutive models, 22–31, 230–250
Contact inhibition, 159–160
Continuum-based models, 275–283
  biphasic model, 282–283
  liquid drop models/cortical shell liquid models, 275–278
  power law structural damping model, 280–282
  solid models, 278–280
    linear elastic solid model, 278–279
    linear viscoelastic solid model, 279–280
Contractile cells, viscoelasticity of, 21

Cortex rheology and delay differential equations, 114–115
Cx43 carboxy-tail, 9
Cytoplasm, 261–262
Cytoskeletal (CSK), 261, 274–275
Cytoskeleton, 86–87

D

Darcy's law, 215–218
Dashpot element, 22–24, 23*f*
Deep cells, 137–139
Delay Differential Equation (DDE), 115
Delayed cell contraction, model of, 212–215
Desmosomal clathrins, 65–66
Desmosomes, 65–66
Dome, 137–139
Doming, 147–148
Drosophila border cells, 3, 91–92
Drosophila embryogenesis, 67–68
Durotaxis, 62, 95–96
  environmental viscoelasticity and, 95–96

E

Ebola virus, 263–264
E-cadherin, 91–92, 149–150, 198–199
Edward's statistic, 228–229
EGF, 178
Elastic deformation, 203–204
Elastic modulus, 209
Elastic potential function, 113
Embryogenesis and wound healing, 90–92
Enveloping layer (EVL), 137–142, 147
Environmental viscoelasticity, 84–93
  cell–cell junctions, modifying, 89–90
  and the control of mesenchymal-to-epithelial transition (MET), 96–97
  cytoskeleton, 86–87
  and durotaxis, 95–96
  focal adhesions (FAs), 85–86
  matching viscoelasticity
    in cancer cells, 92–93
    in embryogenesis and wound healing, 90–92
  nucleus, 87–89
  at the onset of CCM, 94–95
Epiboly, 137–146, 141*f*
Epithelia, actin architecture in, 58–59
Epithelial bridges, 180
Epithelial cell adhesion, 11–12
Epithelial-to-mesenchymal transition (EMT), 6, 92–93, 96–97
Escherichia coli, 263–264
Eukaryotic cells, 276–277
Euler buckling, 54–55
Expanding tissues, elastic behavior of, 179–180
Experimental models to study collective cell migration, 2–7
  in vitro studies, 2–3
  in vivo studies, 3–7, 5*f*
Extracellular matrix (ECM), 47, 51, 59, 80, 85–86, 257, 274–275
Extracellular signal-regulated kinases (ERK) activation, 169–170, 172
Eyring transition state theory, 229

F

F-actin, 54–55
Filopodia, 56–57
Fine-tuning viscoelasticity
  cellular components, viscoelasticity of, 80–84
  collective cell migration, 79–80
    in challenging environments, 80
  environmental viscoelasticity, 93–97
    and the control of mesenchymal-to-epithelial transition (MET), 96–97
    and durotaxis, 95–96
    at the onset of CCM, 94–95
  environmental viscoelasticity, sensing and transducing, 84–93
    cell–cell junctions, modifying, 89–90
    cytoskeleton, 86–87
    focal adhesions (FAs), 85–86
    matching viscoelasticity in cancer cells, 92–93
    matching viscoelasticity in embryogenesis and wound healing, 90–92
    nucleus, 87–89
  future perspectives, 97–98

Finite biointerface, configuration changes of migrating cells for, 236–238
Fluorescence video microscopy, 148–149
Focal adhesions (FAs), 85–86
  based migration, 60–61
Förster resonance energy transfer sensors, 161–162
Fourier integral transform, 25–26
Fourier transform, 22
Four-parameter model, 22, 27–28, 30, 30*f*, 37, 39

G
Gap27 inhibition, 9
Gap junctions (GJs), 8–9, 89–90
Gastrulation, 148–150
Glass micropipettes, preparation and mounting of, 196–197
Global oscillations, 173, 175–176
Glycyrrhizin, 263
Golgi apparatus, 2

H
Heaviside function, 212–213
HeCaT cells, 183
Homotypic channels, 8–9
Hookean behavior, 80–84
Hookean elastic solid, 27–28, 27*f*
Hookean material, 80–84
Hydrogel matrix rheological response, compression caused by, 41
Hyperosmotic stress, cell aggregate under, 40–41

J
Jamming, 160
Jamming state, 31–36
Jamming transitions, 67–68, 68*f*
Jeffreys model, 22, 24, 36–37
  for viscoelastic liquid, 26–27

K
Kelvin–Voigt model, 22, 26–28, 37, 41, 206, 214–215, 281–282

L
Lambert function, 119
Lamellipodium, 58–59
Lamé constants, 282–283
Lamins, 87–88
Laplace's law, 203, 207–209
Laser ablation, 52
Linear delay-differential equation, 115–119
Linear elastic solid model, 278–279
Linearized form, analysis of, 128–130
Linear viscoelasticity, 23–31
  viscoelastic liquid behavior, 24–27
  viscoelastic solid behavior, 27–31
Linear viscoelastic solid model, 279–280
Liquid drop models/cortical shell liquid models, 275–278
Long-time viscoelasticity
  at macroscopic level, 239–250
    configuration changes of migrating cells at a macroscopic level, 241–243
    kinetic constants formulation, 243–246
    mixed series-parallel mode coupling at a macroscopic level, 239–241
    multicellular surfaces, complex modulus of, 246–247
    multicellular surfaces responses under stress conditions, 247–250
  at mesoscopic level, 230–239
    finite biointerface, 235–238
    interface size influences viscoelasticity by mechanical coupling modes, 238–239
    sharp biointerface, 232–235
Loss Modulus, 52–53
Lyme disease, 263–264
Lysophosphatidic acid and its receptor (LPAR2), 90

M
Macroscopic level, long-time viscoelasticity at, 239–250
  configuration changes of migrating cells at macroscopic level, 241–243
  kinetic constants formulation, 243–246

  - mixed series-parallel mode coupling at macroscopic level, 239–241
  - multicellular surfaces, complex modulus of, 246–247
  - multicellular surfaces responses under stress conditions, 247–250
- Madin-Darby Canine Kidney (MDCK) monolayers, 165–167, 166*f*
- Magnetic twisting cytometry (MTC), 266–267, 280–281
- Maxwell model, 22, 24–27, 29–30, 36–37, 42, 207–208, 275–277
- Mechanical and biochemical perturbations, 227, 241, 246–247, 249–250
- Mechanical coupling modes, interface size influences viscoelasticity by, 238–239
- Mechanopharmacology, 263
- Mechanosensitivity, 210, 219–220
- Mechanotransduction, 262–264, 282–283
- Mesenchymal cells, 56–57
- Mesenchymal-to-epithelial transition (MET), 92–93, 96–97
  - environmental viscoelasticity and the control of, 96–97
- Mesodermal progenitor (MSP) zone, 150–152
- Mesoscopic level, long-time viscoelasticity at, 230–239
  - interface size influences viscoelasticity by mechanical coupling modes, 238–239
  - series and parallel mode coupling at mesoscopic level
    - finite biointerface, 235–238
    - sharp biointerface, 232–235
- Microbead rheology, 50–51
- Microbeads, 266–267
- Microelastography, 268–270, 271*f*
- Microfluidic channels, 199–200
- Micropipette aspiration technique, 194–200, 195*f*
  - aggregate preparation, 198–199
  - experimental chamber, 197
  - glass micropipettes, preparation and mounting of, 196–197
  - microfluidic channels, 199–200
  - pressure system, 198
  - video microscopy and image analysis, 199
- Microrheology, 266–268, 268*f*
- Microtubule-organizing center, 2
- Microvilli, 58
- Mitosis, role of, 178–179
- MMP-3 metalloprotease, 92–93
- "Molecular clutch" model, 60–61
- Monolayer stress microscopy (MSM), 161–162
- Morphogen, 157–158
- Morphogenesis and zebrafish development, 137–139
- Multicellular systems, 38–42, 225–227
  - cell aggregate micropipette aspiration, 41–42
  - hydrogel matrix rheological response, compression caused by, 41
  - hyperosmotic stress, cell aggregate under, 40–41
  - long-time rearrangement of multicellular surfaces under external stress, 227–230
  - long-time viscoelasticity
    - at macroscopic level, 239–250
    - at mesoscopic level, 230–239
  - uniaxial compression, aggregate rounding after, 38–40
- Multinodal oscillations, 173
- Multinodal standing waves, 172–177
  - quasi-one-dimensional lines, waves on, 173–175
  - standing waves on extended two-dimensional systems, 175–177
- Murin sarcoma cell aggregates, rheological parameters for, 208–210
- Myosin-2 activity, 55–56

N

- Navier's equation, 284–285
- N-cadherin, 90–91
- *Neisseria meningitidis*, 219
- Newtonian liquid, 24–26, 24*f*
- Newtonian liquid drop, 275–276
- Noninvasive measurement tools, 52

Non-linear form, stability of, 130
Nonlinear viscoelastic solid, characteristics of jamming state as, 31–36
Nuclear lamina, 87–88
Nuclear Lamins. *See* Lamins
Nucleus, 87–89, 262

O

On-plane deformation, 124–126
Optical stretching, 51
Oscillations in collective cell migration, 157
  collective cell motion, mechanism of, 158–160
    density, role of, 159–160
    mechanical machinery, 158–159
  mechanical considerations, 177–181
    affecting the correlation length, 177–178
    cellular level, effective inertia at, 180–181
    expanding tissues, elastic behavior of, 179–180
    mitosis, role of, 178–179
  propagative waves, 160–170
    collective migration with confining borders, 165–168
    colliding tissues, 164
    external boundaries, orientation at, 165
    mechanical forces in expanding monolayers, 161–162
    oscillations in expanding monolayers, 162–164
    velocity oscillations in confined channels, 168–170
  standing waves in fully confined monolayers, 170–177
    breathing oscillations, 170–172
    multinodal standing waves, 172–177
Oscillatory response of cell monolayers, time delays and viscoelastic parameters in, 111
  planar deformations, 112–124
    cortex rheology and delay differential equations, 114–115
    and equilibrium equations, 112–114
    linearized equations of planar deformation, 115–122
    non-linear system of planar deformations, 122–124
  tissue cross-section, analysis of, 124–130
    on-plane deformation, 124–126
    out-of-plane deformation, 126–130
Out-of-plane deformation, 126–130
  linearized form, analysis of, 128–130
  non-linear form, stability of, 130

P

Parallel plate rheometry, 51
Passive microrheology, 266–267
Percolation model, 274–275
Permeability of cellular aggregates, 215–218, 216*f*
Planar deformations, 112–124
  cortex rheology and delay differential equations, 114–115
  linearized equations of, 115–122
    linear delay-differential equations, 115–116
    linear delay differential equation system, solution of, 117–119
    stability and oscillatory analysis of linear delay differential equation, 119–122
  non-linear system of, 122–124
Posterior lateral line primordia (pLLP), 3–6
Power law structural damping model, 280–282
Prechordial plate (ppl), 148–149
Presomitic mesoderm (PSM), 150–152
Pressure system, 198
Propagative waves, 160–170
  collective migration with confining borders, 165–168
  colliding tissues, 164
  external boundaries, orientation at, 165
  mechanical forces in expanding monolayers, 161–162
  oscillations in expanding monolayers, 162–164
  velocity oscillations in confined channels, 168–170

Q

Quasi-one-dimensional lines, waves on, 173–175

R

RAB5, 178
Reslice function, 199
Resting-to-migrating cell state transition, 243–244

S

Sharp biointerface, configuration changes of migrating cells for, 233–235
Shear thinning liquid drop model, 275–276
Shear wave elastography, 268–269
Shivering of cellular aggregate, 210–212, 211*f*
Single cell, rheological modeling of, 272–283
- continuum-based models, 275–283
  - biphasic model, 282–283
  - liquid drop models/cortical shell liquid models, 275–278
  - power law structural damping model, 280–282
  - solid models, 278–280
- structure-based models, 272–275
  - percolation model, 274–275
  - tensegrity model, 272–274, 274*f*

Single-cell migration, actin architecture during, 56–58
Slip bonds, 59
Solid models, 278–280
- linear elastic solid model, 278–279
- linear viscoelastic solid model, 279–280

Somite formation, 150–152
Spherical cellular aggregates, 38
Spring element, 22–24, 23*f*
Spring-pot element, 22, 23*f*, 33, 33*f*
Stability and oscillatory analysis of linear delay differential equation, 119–122
Standing waves, 184–185
Standing waves in fully confined monolayers, 170–177
- breathing oscillations, 170–172
- multinodal standing waves, 172–177
  - quasi-one-dimensional lines, waves on, 173–175
  - standing waves on extended two-dimensional systems, 175–177

State-of-the-art rheology technologies, 271*t*
Steady-state dynamics, 234–235
Storage Modulus, 52–53
Strain rate, 26–27
Strain tensor, 239–241
Stress fibers, 56–57
Stress tensor, 239–241
Structure-based models, 272–275
- percolation model, 274–275
- tensegrity model, 272–274

Studying collective cell migration
- in vitro studies, 2–3
- in vivo studies, 3–7, 5*f*

Subcellular scale measurement tools, 50–51
Substrate mechanics during migration, 61–64
Surface tension, 55–56, 201–203

T

Tensegrity model, 272–274, 274*f*
3D assays, 4*b*
Tight junctions (TJs), 11, 89–90
Timescale-dependent behavior in viscoelastic materials, 48
Tissue cross-section, analysis of, 124–130
- on-plane deformation, 124–126
- out-of-plane deformation, 126–130
  - linearized form, analysis of, 128–130
  - non-linear form, stability of, 130

Tissue mechanics, 194
Tissue mechanosensitivity, 219–220
Tissue-scale measurement tools, 51–52
2D wound healing assay, 4*b*
Tygon tubing, 197

U

Uncorrelated motility, 226–227, 234, 238–239, 241, 246, 251

Uniaxial compression, aggregate rounding after, 38–40
Unsteady-state dynamics, 234

V
Vicsek models, 181
Video microscopy and image analysis, 199
Viscoelastic biological materials, 80–84
Viscoelastic liquid, Jeffreys model for, 26–27
Viscoelastic models, 22
  main characteristics of, 36–38
Viscoelastography, trends in, 283–286
Viscous dissipation, 204–205

W
Whole-cell measurement tools, 51
Wound healing, matching viscoelasticity in, 90–92

X
Xenopus cranial neural crest cells, 3, 6, 90, 94–95
X-waves, 162–164

Y
Yolk–medium interface, 146
Yolk syncytial layer (YSL), 137–139
Young's modulus, 278

Z
Zebrafish blastodermal cells, 90–91
Zebrafish development, 138*f*
  doming, 147–148
  epiboly, 137–146, 141*f*
  gastrulation, 148–150
  morphogenesis and, 137–139
  somite formation, 150–152
Zebrafish lateral line primordia, 3
Zebrafish posterior lateral line primordia (pLLP), 3–6
Zener model, 22, 27–31, 37, 41

Viscoelasticity and Collective Cell Migration

An interdisciplinary perspective across levels of organization

Viscoelasticity and Collective Cell Migration focuses on the main viscoelastic parameters formulated based on multiscale constitutive modeling, and the way how to measure these rheological parameters based on existent micro-devices such as micro-rheology and micro-elastography.

Morphogenetic mechanisms underlying embryonic tissue development, adult tissue homeostasis and regeneration, and cancer are related to multiscale nature of viscoelasticity. This book sheds light on interrelations across viscoelasticity scales, which are essential to reach a deeper understanding of various biomedical processes such as morphogenesis, wound healing, and cancers invasion. Cumulative effects of structural changes at subcellular and cellular levels influence viscoelasticity at a supracellular level. At the same time, established configuration of migrating cells and the rate of its change that significantly influence viscoelasticity at a supracellular level, impact to the cohesiveness inhomogeneity and consequently to various mechanical and biochemical processes at a subcellular and cellular levels.

This book offers deeper understanding of these complex dynamics that represent the challenge and necessity for further development of this field.

The book provides valuable insights for biologists, physicists, engineers, students, and researchers in the field of developmental biology. This is a complex multidisciplinary field, so that perspectives are included from experts in biology, biochemistry, biomedicine, biophysics, and biorheology.

Dr. Ivana Pajic-Lijakovic is a scientific advisor. Her research interest is related to biological physics, biorheology, and biomechanics. She worked as a guest editor for Seminars and Cell and Developmental Biology for the special issue titled: "Viscoelasticity of multicellular systems: from subcellular to supracellular levels."

Elias H Barriga is a group leader at the mechanisms of morphogenesis lab at Instituto Gulbenkian de Ciencia, Portugal. His lab focusses in studying biomechanical and bioelectrical control of collective cell migration in embryo development and regeneration

ISBN 978-0-12-820310-1

9 780128 203101

ELSEVIER

ACADEMIC PRESS
An imprint of Elsevier
elsevier.com/books-and-journals